Lithospheric unzipping explaining hot orogenesis during continental subduction

Douwe J.J. van Hinsbergen[1], Thomas N. Lamont[2], Carl Guilmette[3]

1. Department of Earth Sciences, Utrecht University, Princetonlaan 8A, 3584 CB Utrecht, Netherlands
2. School of Earth Sciences, Wills Memorial Building, University of Bristol, Bristol, 26 BS81RL, UK
3. Département de Géologie et de Génie Géologique, Université Laval, Québec, QC, Canada

Corresponding author: D.J.J. van Hinsbergen, d.j.j.vanhinsbergen@uu.nl

Key Points

-The Aegean-Anatolian orogen contains 20-35 km thick continental nappes that underwent prograde Barrovian metamorphism

-We explain this by lithospheric unzipping at the Moho: the crust underthrusted the upper plate, the mantle lithosphere subducted

-Lithospheric unzipping was the default geological response to continental subduction in the Proterozoic

*THIS MANUSCRIPT HAS NOT BEEN PEER REVIEWED YET.

IT IS SUBMITTED TO 'TECTONICS'.*

ABSTRACT

Accretionary orogens often contain upper crustal nappes derived from subducted continental lithosphere that display (ultra-)high-pressure, low-temperature ((U)HP-LT) metamorphism. Surprisingly, such orogens also contain continent-derived nappes that underwent 'Barrovian' (MP-HT) prograde metamorphism instead. Here, we show that these Barrovian nappes were transported at a low angle below the orogenic crustover 150 km or more within ~10 Ma after the inception of its underthrusting. We show for three Barrovian nappes in the eastern Mediterranean region (Kırşehir Block, Menderes massif, Naxos Basal Unit) that they form the deepest exposed structural levels of the orogen and that they are still underlain by 20-35 km thick crust but not their pre-orogenic lithospheric mantle, which forms part of steeply subducted slabs instead. We propose that these Barrovian nappes were accreted by a process of lithospheric unzipping, whereby during continental subduction the crust decoupled around the Moho and underplated the accretionary orogen at low angle while the mantle lithosphere subducted steeply, as a slab. The unzipped crust, unprotected by mantle lithosphere, heated up quickly as it underthrusted the orogen. We propose that continental subduction has three modes: (i) Formation of thin (U)HP-LT nappes during subduction of stretched continental margins; (ii) underplating of thicker, MP-HT continental crust by unzipping; and (iii) eventual arrest of continental subduction with the arrival of unstretched continent. Finally, the process of lithospheric unzipping may have been the default geological response to continental subduction in a hotter, younger Earth, possibly explaining enigmatic hot Proterozoic orogenesis, such as in the Trans-Hudson orogen of Canada.

PLAIN LANGUAGE SUMMARY

When oceanic plates and continental margins enter subduction zones, they experience rapid pressure increase, but their temperatures rise more slowly, making ‘high-pressure, low-temperature’ conditions. Surprisingly, the deepest rock units of the mountain belt of Greece and Turkey, which contains continental crust that was off-scraped from the subducted ‘Greater Adria’ continent, experienced high temperatures and only medium pressures during their burial. We show here that these rocks were transported at a low angle, and over 150-200 km below the orogen. We explain these observations by a process of ‘lithospheric unzipping’: when thin continental crust enters subduction zones, it is steeply dragged down into a subduction zone, but when thicker crust arrives, it ‘unzips’ from the subducting mantle lithosphere and is shoved at low angle between the upper plate and the underlying hot mantle, causing heating. Recent seismological evidence from the eastern Himalaya caught this process in the act. We show that also older metamorphic rocks of the Himalaya, as well as from the Alps may be explained by lithospheric unzipping. Finally, we show examples from the 2 billion-year-old Trans-Hudson mountain belt of Canada showing that lithospheric unzipping may have been the default response to continental subduction in the hotter, younger Earth.

Introduction

The analysis of metamorphic rocks in orogenic belt provides quantitative constraints on the dynamics of subduction and mountain building processes, and changes therein throughout Earth history (Brown & Johnson, 2018). Rocks that become buried in a subduction zone typically undergo high-pressure metamorphism (HP) due to deep burial, but at relatively low-temperature (LT) because heating of rocks, by conduction and fluid convection, take time (Brown, 1993; Brown, 2007; Jamtveit & Austrheim, 2010). Such HP-LT metamorphism (20-40°C/kbar) is common in accretionary orogens that form by the episodic transfer of rock units within discrete thrust sheets (nappes) from a subducting oceanic or continental lithosphere to an overriding plate lithosphere (Cawood et al., 2009; van Hinsbergen & Schouten, 2021). Contrasting high temperature (HT) metamorphism at moderate pressures (MP) ('Barrovian', ~60-100 °C/kbar) typically post-dates and overprints HP-LT metamorphism and occurs when accreted nappes and thickened crust thermally equilibrate following conduction relaxation of isotherms (typically on tens of millions of years timescales (England & Thompson, 1984; Jamieson et al., 1998; Smye et al., 2011), or when they become disturbed by extension or asthenospheric upwelling (Brown, 1993; 2007; Jolivet et al., 2015; Platt & Vissers, 1989). A well-known accretionary region with HP-LT metamorphic belts, often overprinted by younger Barrovian heating, is the eastern Mediterranean orogen in Greece and Turkey (Jolivet et al., 2003; 2015; Okay & Whitney, 2010) (Figure 1). However, the eastern Mediterranean orogen contains three puzzling cases, where nappes deep in the orogen appear to have escaped the HP-LT stage and underwent prograde Barrovian metamorphism instead, along-strike from nappes that simultaneously experienced HP-LT metamorphic conditions in the same subduction zone.

The eastern Mediterranean orogen contains accreted rock units derived from subducted partly oceanic but mostly continental African plate lithosphere (Lamont et al., 2020a; Schmid et al., 2020; van Hinsbergen et al., 2020). Continental subduction produced regionally extensive nappes (Fig. 1) whose age of burial is well-constrained from their youngest sediments and their oldest metamorphic ages (Jolivet & Brun, 2010; van Hinsbergen et al., 2005a; 2020). Coeval prograde HP-LT and Barrovian metamorphism coexisted within those nappes along-strike in the orogen, on short distances (~100 km), and throughout orogenic history (Figure 1): (i) The eclogite-facies Tavşanlı zone of western Turkey was buried at the same time (90-80 Ma) as the Kırşehir Massif of central Turkey that underwent Barrovian prograde conditions (Mulcahy et al., 2014; Pourteau et al., 2019; van

Hinsbergen et al., 2016; Whitney & Hamilton, 2004); (ii) the Eocene Cycladic Blueschist unit of central Greece was buried at the same time (~55-35 Ma) as the Barrovian Menderes Massif of western Turkey (Bozkurt & Oberhänsli, 2001; Jolivet et al., 2015; Lamont et al., 2023b; Schmidt et al., 2015); and (iii) the HP-LT Phillite-Quartzite and Plattenkalk units of Crete and the Peloponnesos were buried coevally (25-15 Ma) with the prograde Barrovian Basal Unit of Naxos (Jolivet et al., 1996; 2010a; Lamont et al., 2020c; 2023b). Previous explanations for the along-strike differences in prograde metamorphic conditions mostly concentrated on one of the three cases and invoked lateral variation in crustal thickening or thinning, mantle delamination, subduction obliquity, subduction and roll-back rates, or dramatic changes in the subduction zone geometry (slab break-off, transferral of subduction) (Jolivet et al., 2010a; Lamont et al., 2020a; Plunder et al., 2018; van Hinsbergen et al., 2010), but none of these explanations apply to all three cases.

Here, we review the tectonic setting and history of the nappes that underwent these contrasting metamorphic histories. We use the previous conceptual explanations as guide for our review, which concentrates on pressure-temperature-time constraints of the three contrasting metamorphic pairs, identify their structural position in the modern orogenic architecture, the interpreted history of structurally higher units, and their position relative to the subduction zone(s) that accommodated Africa-Europe convergence through time. We aim to develop a concept that may explain all three cases and we will discuss how the eastern Mediterranean cases may help using orogenic geological records in deep geological time to decipher subduction history and evolution.

1. Review

2.1 Plate tectonic setting and regional eastern Mediterranean orogenic architecture

The nappes of the E-W trending eastern Mediterranean accretionary orogen were accreted from now-subducted oceanic and continental lithosphere of the African plate and now form part of the Eurasian upper plate. The timing of peak metamorphism generally gets younger structurally downwards and southwards, and the lithologies associated with each nappe grade from distal oceanic (ophiolite, pelagic sediments) to more proximal continental (shelf carbonates, quartzites and crystalline granitic basement) with increasing structural depth. The orogen is complex, curved, and highly non-cylindrical (van Hinsbergen et al., 2020) (Figure 1). Nappe stacking resulted in significant crustal thickening: in regions unaffected by later extension, the crust is still up to 40-45 km (Abgarmi et al., 2017; Cossette et al., 2016; McPhee et al., 2022). However, this thick crust is underlain by only a thin mantle lithosphere (Abgarmi et al., 2017; Barazangi et al., 2006; Endrun et al., 2011; McPhee et al., 2022). This is likely because the original, pre-orogenic lithospheric underpinnings that existed below the nappes has subducted (Handy et al., 2010; Jolivet & Brun, 2010; van Hinsbergen et al., 2005a; 2010): these subducted underpinnings now forms slabs that are well-imaged with seismic tomography as coherent bodies of lithosphere that penetrate as deep as the mid-mantle (Berk Biryol et al., 2011; Hafkenscheid et al., 2006; van Hinsbergen et al., 2005a).

The curvature of the modern nappe stack is partly the result of the non-cylindrical pre-orogenic paleogeographic distribution of oceanic and continental lithosphere (van Hinsbergen et al., 2020), and partly of the formation of large extensional windows in the center of the orogen (Gürer et al., 2018; Jolivet & Brun, 2010). These extensional windows exhumed and expose the metamorphic rock units discussed in this paper (Figure 1). These windows formed by upper plate extension above the subduction zone that consumed African lithosphere, during Cretaceous to Eocene time in Central Turkey (Gürer et al., 2018) and since the Eocene in western Turkey and Greece (Bozkurt & Oberhänsli, 2001; Jolivet & Brun, 2010) (Figure 1). The Cretaceous nappes discussed in this paper accreted first below an oceanic plate of the Neotethys ocean whose remains are preserved as ophiolites (Gürer et al., 2016; Şengör & Yilmaz, 1981). These ophiolites have a supra-subduction zone geochemistry, have metamorphic soles, and are of Cretaceous age (Lamont et al., 2020a; Parlak, 2016; van Hinsbergen et al., 2016). They are interpreted to represent the remains of an oceanic plate that was above a subduction zone that ended in a triple junction around the Greece-Turkey border and extended southeastward through the Neotethyan Ocean towards the Indian Ocean (van Hinsbergen et al., 2021). This oceanic plate was itself subducting below Europe and was in western and central Turkey fully consumed in the latest Cretaceous (Kaymakci et al., 2009; Mueller et al., 2019; Ocakoğlu et al., 2019), after which accretion occurred directly below the Eurasian plate margin (van Hinsbergen et al., 2020) (Figure 1). The nappes discussed in this paper formed in the western and southeastern branches of this subduction system, that remain active today as the Hellenic and Cyprus trenches.

2.2 Nappes with synchronous but contrasting prograde metamorphic histories

2.2.1 Tavşanlı Zone versus the Kırşehir Block

The Tavşanlı Zone of NW Turkey is a 300 km long and 50 km wide belt of thrusted, blueschist to eclogite-facies, Paleo- and Mesozoic metapelitic schists, metavolcanics, and marbles derived from the now-subducted passive Greater Adriatic continental margin (Okay, 2002) (Figure 1), overlain by unmetamorphosed ophiolites that are likely similar in age as the underlying metamorphic sole hornblende $^{40}Ar/^{39}Ar$ cooling ages of 93-90 Ma (Önen, 2003; Önen & Hall, 1993). The Tavşanlı Zone became buried to pressures up to 24 kbar at temperatures up to ~500°C (~20°C/kbar) (Davis & Whitney, 2008; Okay, 2002; Plunder et al., 2013) (Figure 2). Lu/Hf geochronology on garnet and lawsonite gave ages interpreted as the timing of burial metamorphism was 91-83 Ma (Mulcahy et al., 2014; Pourteau et al., 2019), showing that subduction of the Tavşanlı Zone occurred soon after, or even partly during SSZ ophiolite spreading in the upper plate. The Tavşanlı Zone is a few km thick and overlies a younger passive margin-derived nappe, the Afyon Zone, metamorphosed at ~10 kbar/350-400°C (~35-40°C/kbar) around 70-65 Ma (Pourteau et al., 2013), following ~15 Ma of subduction without accretion (van Hinsbergen et al., 2016). The Tavşanlı Zone was slowly exhumed and became eventually intruded by arc plutons of 60-50 Ma, in places associated with a Barrovian (MP-HT) metamorphic overprint (Seaton et al., 2014). These arc plutons formed after the Afyon Zone accreted and the trench consequently had stepped southwards, moving the Tavşanlı Zone into the arc position, ~30-40 Ma after its initial underthrusting and accretion.

To the east and southeast of the Tavşanlı Block, the Kırşehir Block of central Turkey exposes greenschist to granulite-facies, Paleo-Mesozoic metapelites, metavolcanics, and marbles overlying a Precambrian crystalline basement (Whitney & Hamilton, 2004). The Kırşehir Block was buried below oceanic lithosphere preserved as the Central Anatolian supra-subduction zone ophiolites (Floyd et al., 2000), with U/Pb zircon plagiogranite ages of 90.5 ± 0.2 Ma and 89.4 ± 0.6 Ma (van Hinsbergen et al., 2016). The Kırşehir Block now consists of three submassifs separated by fault zones that accommodated shortening and strike-slip and that were rotated relative to each other in Cenozoic time to form a NW-ward convex orocline (Advokaat et al., 2014; Lefebvre et al., 2013). When this orocline is restored, the Kırşehir Block formed a ~150 km wide (E-W) to ~500 km long (N-S), elongated block. During regional amphibolite-facies metamorphism, a pervasive, flat-lying foliation formed that systematically recorded top-to-the-SSW sense of shear (Lefebvre, 2011; Lefebvre et al., 2013). Metamorphic conditions in the Kırşehir Block reached peak pressures of 7-8 kbar at temperatures of ~700

°C (~95°C/kbar) in the central of the three sub-massifs, and 5-6 kbar at 700°C (125°C/kbar) in the southern (Lefebvre et al., 2015; Whitney & Dilek, 1998; Whitney & Hamilton, 2004; Whitney et al., 2003) (Figure 2). There is no evidence for a preceding HP-LT metamorphic phase. U/Pb geochronology on zircon and monazite in migmatites yielded 90-85 Ma ages (Whitney & Hamilton, 2004; Whitney et al., 2003), i.e. partly overlapping with those the overlying SSZ ophiolites, indicating that the Kırşehir Block underthrusted and reached peak metamorphic conditions during upper plate extension.

The restored regional top-to-the-SSW sense of shear during underthrusting if the Kırşehir Block below the Central Anatolian Ophiolites is parallel to the Africa-Europe convergence direction in this time interval and is thus consistent with deformation during burial (van Hinsbergen et al., 2016). The regional foliation of the Kırşehir Block is cut by a belt of undeformed granitic and gabbroic plutons which have U-Pb zircon ages from 85-70 Ma and geochemical signatures that show that they resulted from both mantle derived arc magmatism and crustal melting (Ilbeyli, 2005; Köksal et al., 2004; van Hinsbergen et al., 2016). The intrusion of the arc plutons led to local contact metamorphism (3-4 kbar, ~800°C (Lefebvre et al., 2015) superimposed on regional metamorphism and associated pervasive deformation fabrics. This arc is interpreted to have formed during oceanic subduction that initiated immediately after the Kırşehir Block stopped underthrusting and accreted to the overriding oceanic plate lithosphere (Ilbeyli, 2005; Köksal et al., 2004). This suggests that the Kırşehir Block underthrusted at low-angle over a large distance (the reconstructed arc-trench distance at 85-70 Ma was ~175 km (van Hinsbergen et al., 2020)), so that a slab providing fluids for arc melting must have been present underneath the block when it stopped underthrusting (van Hinsbergen et al., 2016).

After accretion, the Kırşehir Block exhumed along extensional detachments between 85 and 70 Ma. Interestingly, these detachments accommodated E-W extension, i.e. at high angles to the underthrusting direction (Advokaat et al., 2014; Isik et al., 2008; Lefebvre et al., 2011; 2015), but perpendicular to the reconstructed trench orientation at which the Kırşehir Block underthrusted (van Hinsbergen et al., 2016). E-W extension in the upper plate above this evolving N-S trending subduction segment has been pervasive throughout its history: the reconstructed paleo-orientation of sheeted dykes in the Central Anatolian and surrounding ophiolites was N-S, suggesting E-W spreading even shortly after subduction initiation (Maffione et al., 2017; van Hinsbergen et al., 2016), E-W extension continued also after accretion of the Afyon Zone controlling exhumation into the Paleogene (Gürer et al., 2018) and even affected the Neogene basins in the central Taurides (Koç et al., 2017).

The crust of the Kırşehir Block has a present day thickness of ~35 km (Tezel et al., 2013). The Block underwent some thickening due to Oligocene shortening (Advokaat et al., 2014; Gülyüz et al., 2013; Lefebvre et al., 2013), but upper Cretaceous sediments that overlie the Kırşehir Block are terrestrial, showing that its crust after accretion was likely tens of km thick even during regional extensional exhumation (Advokaat et al., 2014). There are no tectonic windows in the Kırşehir Block that show that the younger nappes of the Afyon Zone and the Taurides that fringe the Kırşehir Block to the south (McPhee et al., 2018; Okay et al., 1996) regionally underlie the block. It is thus likely that most if not all pre-orogenic crust of the Kırşehir Block accreted and escaped subduction. After 85 Ma, subduction and arc magmatism continued, without accretion, until underthrusting of the Afyon zone around 70-65 Ma (Pourteau et al., 2013; van Hinsbergen et al., 2016). The Afyon zone accreted against the Kırşehir Block and Tavşanlı zone to the south, i.e. some 15 Ma after their climax metamorphism, and the Afyon zone was everywhere metamorphosed under similar HP-LT conditions (~35-40 °C/kbar) with no significant along-strike variation (Candan et al., 2005; Pourteau et al., 2010; 2013). After accretion of the Afyon Zone, and during the formation of the Tauride fold-thrust belt to the south, upper plate extension continued and widespread sedimentary basins formed in which terrestrial to shallow marine sedimentation occurred in Paleocene-Eocene time (Gürer et al., 2016; 2018; Seyitoğlu et al., 2017).

2.2.2 Cycladic Blueschist versus Menderes Massif

The Cycladic Blueschist (CBS) comprises a series of nappes that collectively represent a few km structural thickness and that is exposed on the Cycladic Islands and on the Aegean mainland (Jolivet & Brun, 2010; Schmid et al., 2020). The upper parts of the CBS are oceanic crust-derived and comprise metabasites enclosed in serpentinite, which overthrust nappes consisting of a Palaeozoic crystalline basement overlain by Triassic mafic volcanics, and a metasedimentary sequence of presumably deep-marine origin (Bröcker & Pidgeon, 2007; Kotowski & Behr, 2019). The continental CBS is correlated with the pelagic carbonates and cherts of the Pindos Zone of the external Hellenides that was underlain by strongly thinned continental lithosphere (Schmid et al., 2020). In the western Cyclades, the CBS is overlain by the Pelagonian continental nappe that extend towards the Dinarides; in the central and eastern Cyclades, the highest structural units are Middle Jurassic ophiolites that regionally obducted the Pelagonian zone during the Early Cretaceous, but that in the central Cycladic region remained in an intra-oceanic position until the Late Cretaceous, after which the CBS underthrusted (Lamont et al., 2020a; Schmid et al., 2020). This difference in obduction age is interpreted as a result of lateral variations in the paleogeography of the upper plate during CBS subduction (Lamont et al., 2020a; van Hinsbergen et al., 2020). The CBS overlies the Basal Unit which includes a continental plate stratigraphy with Paleozoic crystalline basement, passive margin meta-clastics and volcanics, a marble platform sequence, and an Oligocene meta-foreland basin sequence (Schmid et al., 2020) and references therein). The Basal Unit thus underthrusted the CBS in Oligocene to Early Miocene time (Lamont et al., 2023b; Ring et al., 2007a; Schmid et al., 2020). We will return to the Basal Unit in the next section.

The CBS nappes experienced blueschist to eclogite-facies metamorphism (18-23 kbar, 500-600°C, ~20-30 °C/kbar) (Behr et al., 2018; Lamont et al., 2020b; Laurent et al., 2017; Skelton et al., 2019; Wolfe et al., 2023) (Figure 2) and returned U/Pb and Lu/Hf ages between ~55-38 Ma, of which the rocks with continental protoliths recorded ages from ~48 Ma onwards (Dragovic et al., 2012; Gorce et al., 2021; Kotowski et al., 2022; Lagos et al., 2007; Lamont et al., 2023b; Peillod et al., 2017; Tomaschek, 2003; Tual et al., 2022; Uunk et al., 2022), younging structurally downwards (Kotowski et al., 2022). The first phase of regional exhumation of the CBS, during which it was in places retrogressed under greenschist-facies conditions, occurred between ~35 and 20 Ma while the CBS was being underthrusted by the Basal Unit (Cisneros et al., 2021; Jolivet & Brun, 2010; Lamont et al., 2023b; Ring et al., 2007a; Searle & Lamont, 2020). During much of the underthrusting of the CBS, there was no arc magmatism, which only commenced around ~35 Ma in northern Greece and southern Bulgaria after a lull since the late Cretaceous (Schmid et al., 2020). Upon ongoing nappe accretion and upper plate extension, the arc migrated southwards and arrived in the CBS region around 7 Ma (Ersoy & Palmer, 2013). Around ~15-12 Ma, plutons had already intruded both the CBS and Basal Unit, but these related to crustal melting, and caused local contact metamorphism (Jolivet & Brun, 2010; Jolivet et al., 2003; Lamont et al., 2023b).

To the east of the Cyclades, a series of Eocene metamorphosed nappes is exposed in western Turkey, which were underthrusted below the Afyon Zone (Fig 1). These are exposed in the Menderes Massif, a major extensional window that separated the deeper-buried, HP-LT metamorphic Afyon and Tavşanlı zones to the north from their shallower-buried, lower-pressure to non-metamorphic equivalents, the Lycian Nappes (Collins & Robertson, 2003;

Schmid et al., 2020) (Figure 1). The highest nappe of the Menderes Massif is the Dilek Nappe that contains a passive margin sequence and that underwent comparable, HP-LT metamorphic conditions as the CBS (500°C/15 kbar; ~30°C/kbar) (Rimmelé et al., 2003; Ring et al., 2007b), but only represents the older part of the CBS metamorphic age spectrum, from 52-46 Ma (Pourteau et al., 2013). The deeper part of the nappe stack in western Turkey consists of the Menderes Nappes, which contain Precambrian crystalline basement and a Paleozoic to Eocene meta-clastic and meta-carbonate sedimentary series with platform carbonate fossils (nummulites, rudists) (Bozkurt & Oberhänsli, 2001; Gessner et al., 2001; Özer & Sözbilir, 2003; Schmid et al., 2020). Between ~46 and 35 Ma, the Pindos and Menderes nappes thus underthrusted and metamorphosed simultaneously, side by side in the same subduction zone. Their strong lithological differences are paleogeographic in origin: the shallow-water Menderes platform was bounded to the west by a slope, likely representing a transform fault margin that formed during Triassic Neotethys rifting (van Hinsbergen et al., 2020).

The Menderes Nappes escaped HP-LT metamorphism and instead experienced Barrovian prograde metamorphism, with peak metamorphism estimated at up to ~500-550°C at 6-8 kbar (60-90 °C/kbar) (Okay, 2001; Whitney & Bozkurt, 2002) (Figure 2), although other parts remained at greenschist facies conditions (Gessner et al., 2001). Lu/Hf garnet growth ages show prograde mineral growth between ~42 and 35 Ma (Schmidt et al., 2015), consistent with Rb-Sr ages (Bozkurt et al., 2011) and ^{40}Ar-^{39}Ar syn-metamorphic ages of greenschists (Lips et al., 2001), i.e. overlapping with the younger part of the CBS HP-LT age spectrum spanning ~55-40 Ma. Within a few Ma after accretion of the Menderes Nappes, late Oligocene arc volcanism occurred in the hanging wall of the north-dipping detachments that exhumed the northern Menderes Massif (Ersoy & Palmer, 2013), showing that the massif underthrusted the entire west Anatolian forearc. The massif is intruded by granitoids that bear similarities to arc magmas (Akay, 2009; Ozgenc & Ilbeyli, 2008), with ages of ~23-20 Ma (Isik et al., 2004; Ring & Collins, 2005).

The Menderes Massif is still underlain by ~30 km thick continental crust (Tezel et al., 2013) and is likely the contiguous with the Bey Dağları platform that is located in the non-metamorphic foreland, to the south of the Lycian Nappes klippe (Figure 1). After ~35 Ma, convergence became accommodated at the Hellenic-Cyprus trench to the south of the Bey Dağları platform, consuming oceanic lithosphere of the Eastern Mediterranean Ocean basin, which no exposed accretionary record (van Hinsbergen et al., 2020). Seismic tomographic images of the mantle below western Anatolia reveal a single slab, which detached likely in Miocene time (Jolivet et al., 2015; van Hinsbergen et al., 2010), that must account for subduction since the Cretaceous. To explain the present crustal thickness of western Turkey, most of the west-Anatolian crust likely consists of the pre-orogenic continental crustal underpinnings of the deepest Menderes units that decoupled from their subducted mantle lithospheric underpinnings (van Hinsbergen et al., 2010).

2.2.3 Phillite Quartzite/Plattenkalk Units versus Naxos Basal Unit

The Phyllite Quartzite unit (PQ) and the underlying Plattenkalk unit are exposed on Crete and the Peloponnesos and are the youngest HP-LT metamorphic nappes of the eastern Mediterranean orogen (Jolivet et al., 1996; Jolivet et al., 2010a; Theye et al., 1992). The structurally higher PQ nappe is a few km thick and comprises thin slivers of Paleozoic crystalline basement (Romano et al., 2004) overlain by a Carboniferous to Triassic meta-clastic sedimentary series (Krahl et al., 1983) interpreted to reflect a continental passive margin sequence (Schmid et al., 2020). The unit is interpreted to have been the stratigraphic base of the Tripolitza platform carbonates that are structurally above the PQ units, and which stratigraphically span the Triassic to Eocene (van Hinsbergen et al., 2005b). The Tripolitza Nappe underlies the Pindos Nappe (i.e., the metamorphic equivalent of the Cycladic Blueschist unit). The current contact between the HP-LT PQ Unit and the anchi-metamorphic Tripolitza limestones is an extensional detachment that accommodated part of the exhumation of the PQ Unit (Jolivet et al., 1996; Rahl et al., 2005). The PQ was buried to up to 18 kbar at ~400°C around 24-20 Ma (~20°C/kbar) (Jolivet et al., 1996; Jolivet et al., 2010a) (Figure 2). The PQ was thrust upon the Plattenkalk Unit that consists of a Triassic to Oligocene stratigraphy of deep-marine meta-clastic and -carbonate sediments and foreland basin clastics that reached metamorphic conditions of 7-8.5 kbar at 310-360°C (20-50°C/kbar) on the Peloponnesos (Blumor et al., 1994). The Plattenkalk Unit is correlated to the Ionian zone of the non-metamorphic Aegean foreland (Blumor et al., 1994; Schmid et al., 2020). Because the Plattenkalk Unit reached lower peak-pressure conditions than the overlying PQ unit, part of the exhumation of the PQ must have occurred during the underthrusting of the Plattenkalk. This is interpreted to have occurred in a subduction channel or extrusion wedge setting along the plate contact, accommodated along detachments at the top of the PQ (Fassoulas et al., 1994; Laurent Jolivet et al., 2003; L. Jolivet et al., 1996; Uwe Ring & Yngwe, 2018; Thomson et al., 1999).

Since ~15 Ma, exhumation was further aided by multidirectional forearc thinning during oroclinal bending (Douwe J. J. van Hinsbergen & Schmid, 2012), to reach near-surface conditions in the late Middle Miocene (Marsellos et al., 2010) and first exposure around 10 Ma (Zachariasse et al., 2011).

Field geological and seismic observations in the foreland of western Greece and the Peloponnesos showed that the underthrusting of the Tripolitza Nappe (and its PQ stratigraphic underpinnings) below the Pindos Nappe, and of the Plattenkalk/Ionian nappes below the Tripolitza Nappe started simultaneously, around 35 Ma (IGRS-IFP, 1966; Sotiropoulos et al., 2003; Douwe J. J. van Hinsbergen & Schmid, 2012). Underthrusting of the Tripolitza/PQ ended in the earliest Miocene, but for the Ionian zone continued until the late Miocene. Subsequently, the subduction plate contact stepped structurally downward towards the modern Hellenic Trench south of Crete where the thick 'Mediterranean Ridge' accretionary prism formed (Kastens, 1991), and structurally deeper into the Adriatic continental foreland in western Greece where the Pre-Apulian nappe accreted (D. J. J. van Hinsbergen et al., 2006). The Phyllite-Quartzite unit is still located in the Aegean forearc, >100 km to the south of the active arc (Figure x).

To the north, on the islands of e.g. Evia (Ring et al., 2007a), Samos (Gessner et al., 2011), and Naxos (Lamont et al., 2020a; 2023b), the Basal Unit is exposed in windows below the Cycladic Blueschist Unit, as deepest exposed structural nappe of the Cyclades. The Basal Unit's proximal, shallow marine meta-platform carbonates with bauxite horizons (interpreted to be paleosol erosional surfaces) with stratigraphic ages that extend into the Eocene, and in places Oligocene foreland basin clastics (Ring & Layer, 2003) is correlated to the unmetamorphosed Tripolitza platform carbonates in the Aegean foreland (Schmid et al., 2020). On Evia and Samos, the Basal Unit reached pressures of ~8 kbar at ~400°C (50°C/km) between 20 and 15 Ma (Ring & Layer, 2003; Ring et al., 2001), but in the heart of the Cycladic extensional province on Naxos, where Miocene extension was most maximal (Jolivet et al., 2010b; van Hinsbergen & Schmid, 2012), the Basal Unit underwent much hotter prograde metamorphism instead, reaching Barrovian conditions of ~10-11 kbar and ~600-730°C (i.e., 55-73°C/kbar) (Figure 2) dated by U-Pb zircon at 20-16 Ma (Lamont et al., 2020a; 2023b). This was followed by partial melting, isothermal decompression and a lower pressure sillimanite grade overprint (5-6 kbar and 670-730°C) at ~16-14 Ma (Lamont et al., 2023b; Ring et al., 2007a; Schmid et al., 2020) and intrusion if crustal derived granites at ~15-12 Ma

(Jolivet & Brun, 2010; Jolivet et al., 2003; Lamont et al., 2023a). In other words, burial of the Basal Unit occurred at the same time as the PQ and Plattenkalk units to the south and may even have continued while the PQ was already exhuming above the downgoing Plattenkalk unit.

The Basal Unit was buried by underthrusting while the Cycladic Blueschist was exhuming and retrogressed, bounded at the top by an extensional detachment (Jolivet et al., 2003; Lamont et al., 2020a; 2020c; 2023b; Ring et al., 2007a; b; Searle & Lamont, 2020). Moreover, exhumation along extensional detachments and associated supra-detachment extensional basins had already been occurring farther north in the Rhodope region since the Eocene, and was continuing throughout the Miocene (Brun & Sokoutis, 2007; 2010), showing that the low-angle underthrusting of the Basal Unit belof the forearc occurred while the overriding plate was in extension. Around 15 Ma, when underthrusting of the Basal Units stopped, it also became exhumed by low-angle normal faults as evidenced by the extreme telescoping of metamorphic stratigraphy and isograds in Western Naxos immediately beneath the Naxos-Paros Detachment (Lamont et al., 2023a).

The present-day Moho depth below the Cyclades is 25-26 km (Cossette et al., 2016). Around 15 Ma, the Basal Unit and Cycladic Blueschist Unit became intruded by I-type and S-type granitic plutons (Altherr et al., 1988). When their extensional exhumation is restored, the Basal Unit (and Cycladic Blueschist Units and associated granites) restore below the northern Aegean and NW Anatolian portions of the orogen, >200 hundred km north of the trench at which it underthrusted (van Hinsbergen & Schmid, 2012). Such a large low-angle underthrusting of the Basal Unit/Tripolitza Unit occurred regionally: also in a structural window in the cores of Mount Olympos and Mount Ossa on eastern Mainland Greece, the Basal Unit is exposed, some 140 km from the trench at which the Tripolitza Unit underthrusted the Aegean orogen (Schmid et al., 2020; van Hinsbergen & Schmid, 2012).

The continental crust that melted to form the I- and S-type granites of the Cyclades (Lamont et al., 2023a), is likely the 25-26 km thick crust that still underlies the Cyclades (Tirel et al., 2004). Schmid et al. (2020) inferred that crust must somehow have accreted from the subducted African Plate and suggested that it all consists of Ionian (Plattenkalk) crust, which structurally underlies the Tripolitza/PQ units in the external Hellenides and Crete. The Ionian Zone should then have underthrusted most of the Aegean region in tandem with the Tripolitza/Basal Unit. Alternatively, Lamont (2020a; 2023b) and Searle & Lamont (2020) suggested that the Basal Unit is still underlain by its own pre-orogenic crust, and they interpreted that this marks a phase of subduction transferral, with a subducting slab breaking off the Basal Unit lithosphere and a new subduction zone starting to the south. In any case, the crustal thickness of Greece requires that the deepest nappe of the orogen still contains (most of) its original, pre-orogenic crust.

2. Discussion

3.1 Lithospheric unzipping

The three case studies above from the Cretaceous to Cenozoic eastern Mediterranean accretionary orogen show that at the same time, and at the same subduction zone, regionally extensive rock units may underthrust at contrasting angles and geothermal gradients and thus experience contrasting prograde metamorphic evolutions. We identify some key differences between the HP-LT metamorphic units that were buried to depths of up to ~20 kbar under net geothermal gradients of ~20-40 °C/kbar, and the Barrovian units that were buried to pressures of no more than ~8-11 kbar under geothermal gradients of ~60-100°C/kbar.

The HP-LT units (Tavşanlı, Afyon, Cycladic Blueschist, Phyllite-Quartzite/Plattenkalk Units) are thin nappes, no more than a few km thick, consisting mostly of deep-marine sedimentary cover units of thinned continental margin lithosphere, only occasionally still including small fragments of the originally underlying crystalline basement. These HP-LT nappes underwent rapid burial, shown by time gaps between the youngest stratigraphic ages and the oldest metamorphic ages of only ~10 Ma, and rapid subsequent exhumation, whereby during their exhumation, they thrusted over simultaneously underthrusting younger nappes (Ring et al., 2007a; Searle & Lamont, 2020). The HP-LT nappes may be intruded by arc-derived, or crustal melting-derived plutons, but only after a new forearc crust was built between the HP unit and the trench, tens of Ma after HP metamorphism. Such histories of rapid burial and exhumation close to subduction zones have long been recognized and are most commonly explained by buoyancy-driven rise (or tectonic extrusion (Ring & Yngwe, 2018)) in a subduction channel (Brun & Faccenna, 2008; Jolivet et al., 2003; Platt, 1986; Thomson et al., 1999).

The Barrovian units (Kırşehir Block, Menderes Massif, Naxos Basal Unit) are all consisting of continental crustal units overlain by shallow-marine carbonate successions. All three units are associated with a crystalline basement, an underlying crust that is still ~25-35 km thick despite widespread extension, and for none of these units evidence exists that this crust consists of younger accreted nappes. Instead, it appears more likely that this crust still consists of the original pre-orogenic continental crust (Searle & Lamont, 2020; van Hinsbergen et al., 2010; 2016) (Figure 1). However, this crust is no longer attached to its (original) mantle lithosphere that appears to have subducted (van Hinsbergen et al., 2010). The Barrovian units and their underlying crust underthrusted at a low angle below the overriding plate, which may consist of previously accreted nappes, in the case of the Naxos Basal Unit and the Menderes nappes, or of oceanic lithosphere of the Central Anatolian Ophiolites in the case of the Kırşehir Massif. Kinematic reconstructions of the orogenic architecture (van Hinsbergen et al., 2020) shows that underthrusting of the Barrovian units below the upper plate was a regional feature: it occurred over 150 km or more across-strike of the reconstructed paleo-trench (Figure 1), so far below the upper plate that it must have been present below the entire forearc. Importantly, in the Aegean and western Anatolian cases, the magmatic arcs remained active during horizontal underthrusting, either stable or migrating in the direction of the trench. For the Kırşehir Massif, arc magmatic plutons intruded the massif within a few Ma after underthrusting, and collectively, the three cases suggest that horizontal underthrusting occurred above a normally dipping slab: a flat slab would have shut off the arc, or led to migration inboard. During the underthrusting, the exposed parts of the Barrovian units reached pressures of no more than ~8-11 kbar but at high temperatures reaching anatexis. Stratigraphic constraints show that this burial and prograde metamorphism occurred within ~10-15 Ma after arrival of the continental unit at the trench, i.e. within the same period as the HP-LT units elsewhere at the same trench. Finally, and paradoxically, underthrusting and prograde metamorphism of the Barrovian units occurred while upper plate was undergoing extension: Oligocene-middle Miocene underthrusting of the Basal Unit occurred while the northern Aegean region underwent extension, and underthrusting of the Kırşehir Block occurred while there was upper plate oceanic spreading forming the Central Anatolian Ophiolites in Central Anatolia. This shows that the low-angle underthrusting of the Barrovian Units below the upper plate may occur while there is net divergence between the trench and the upper plate, either by roll-back or the retreat of the upper plate away from a mantle stationary trench, or both (van Hinsbergen & Schmid, 2012).

These contrasting prograde metamorphic and tectonic histories occurred simultaneously, along-strike in the Cretaceous for Kırşehir vs. Tavşanlı and the Eocene for the Menderes Massif vs. the Cycladic Blueschist, and across-strike in the Oligocene-early Miocene for the Naxos Basal Unit and the Phyllite-Quartzite Unit. To explain these contrasting histories, and the paradox of upper plate extension simultaneously with low-angle underthrusting of continental crust below the entire forearc over a distance of 150 km away from the paleo-trench (Figure 1), we propose that the prograde Barrovian metamorphic units may be explained by a scenario of 'lithospheric unzipping' (Figure 3).

The majority of continent-derived nappes, including those with HP-LT metamorphism, consist of only the sedimentary cover with occasional basement relics, showing that the original continental crystalline crust and mantle lithospheric underpinnings can be dragged down into subduction zones (Handy et al., 2010; Jolivet & Brun, 2010; van Hinsbergen et al., 2005a). The sedimentary facies of the HP-LT metamorphic nappes in the eastern Mediterranean show deep-marine facies and reconstruction places them at microcontinental margins (Tavşanlı, Afyon zones, PQ) or in grabens between horsts (CBS), suggesting that the original underlying continental crust was thinned. With the lithospheric unzipping concept, we postulate that when thicker continental crust enters the trench during continental subduction, such that its buoyancy resists subduction, and/or its strength resists bending, it will no longer be dragged down into the subduction zone, yet it will not stop lithospheric subduction either. Instead, the crust decouples from the lithospheric mantle around Moho depth during descent. This decoupling horizon forms a subhorizontal tear that propagates into the downgoing plate as its subduction continues (Figure 3), gradually and diachronically 'unzipping' the crust from the mantle lithosphere. In the case of the eastern Mediterranean examples, the underplated crust is still up to 35 km thick, which provides a maximum thickness for the original crustal thickness depending on the amount of shortening and thickening during underthrusting. All three examples of the Kırşehir Block, the Menderes Massif, and the Basal Unit, contain shallow marine platform carbonates suggesting that their original crustal thickness exceeded that of the HP-LT metamorphic units.

This process of decoupling may utilize the same rheological contrast that permits delamination by peeling mantle lithosphere from a plate (Göğüş & Pysklywec, 2008; Memiş et al., 2020). Such peeling delamination is known to occur at within-plate settings (Göğüş & Ueda, 2018a), at former subduction zones where plate convergence has stopped, such as in the SW Carpathians and in the Antalya region (Göğüş et al., 2016; McPhee et al., 2019), and subducting slabs may trigger delamination of lithosphere at slab edges (Spakman & Hall, 2010; van de Lagemaat et al., 2021). With 'unzipping', we mean that delamination occurs in the downgoing plate lithosphere during its descent into a subduction zone, and the arrest of this process coincides with the final accretion of the crust to the upper plate. The downgoing plate continental crust is coherent, buoyant, and strong and as long as it remains coupled with the downgoing plate, it is pushed between the base of the upper plate lithosphere and the underlying mantle wedge, at a low angle (Figure 3). In the case of an accretionary orogen such as in western Turkey and Greece, this upper plate lithosphere consists only of accreted, thin supracrustal nappes that were stripped from their pre-orogenic crystalline crustal and mantle lithospheric underpinnings. The deeply buried portions of these nappes that experienced HP metamorphism and subduction channel exhumation before the onset of lithospheric unzipping (e.g., Cycladic Blueschist Unit, Dilek Nappe, and overlying Afyon and Tavşanlı zones) are in direct thrust contact with the underthrusting unzipped crust. In the case of the Kırşehir massif, there were no previously accreted nappes and underthrusting occurred below a thin veneer of subducted oceanic lithosphere-derived subduction mélange and the overlying mantle rocks of the Central Anatolian Ophiolites.

Because the underthrusting crust unzipped from the original mantle lithosphere and is pushed between the hot mantle wedge and the base of the upper plate, it becomes quickly heated from below (in our case studies within 10 Ma after subduction), i.e. at time scales that are much shorter than conductive relaxation of isotherms following crustal thickening (typically 10's Ma; England & Thompson, 1984) while its buoyancy prevents it from sinking. This may explain the rapid prograde HT-MP 'Barrovian' metamorphism during burial. At the same time, subduction of lithospheric mantle continues as a coherent slab. This lithospheric mantle slab continues to hydrate the overlying asthenospheric mantle wedge and if the low-angle underthrusting, unzipped crust reaches the position of the volcanic arc, it may become intruded by arc magmas. In our case studies, where subduction rates were on the order of 2-4 cm/a (van Hinsbergen et al., 2020), and with an arc-trench distance of ~150 km (Figure 1), the position of the arc may be reached within 4-8 Ma after entering the subduction zone, but with higher convergence rates, this time gap may be even shorter. Moreover, if there is divergence between the slab and upper plate, because of slab roll-back or upper plate escape, low-angle underthrusting of unzipping crust may still occur, as it is entirely driven by the subduction of the downgoing plate (Figure 3). This explains the apparent paradox of upper plate extension during continental crustal underthrusting below the extending forearc, as shown for the Cretaceous Central Anatolian and Oligocene-early Miocene Aegean examples. Notably, in western Turkey and Greece, the unzipping occurs after a period of accretion of the only sedimentary cover units, whereby the (thinned) crystalline continental crust and lithosphere are subducted (Jolivet & Brun, 2010; van Hinsbergen et al., 2005). However, when the entire continental crust is accreted through unzipping, the subducting lithosphere only consists of dense, cool lithospheric mantle rocks with a lesser resistance to bending than a full lithospheric section. We speculate that this may accelerate or initiates slab roll-back during unzipping and continental crustal underplating. This may explain why the Mediterranean region has widespread upper plate extension during continental subduction (van Hinsbergen & Schouten, 2021; van Hinsbergen et al., 2020). Finally, the underthrusting of a buoyant crust without its dense underpinnings may cause uplift or shorten the forearc even if the trench and upper plate diverge. In the three cases discussed in this paper, this is not straightforwardly tested: there is a sparse stratigraphic oceanic record and no detailed bathymetric estimate of the Central Anatolian ophiolites. It is possible that such uplift was recorded in the forearcs of western Turkey (in the Lycian Nappes) and Greece (e.g., in the Mesohellenic Basin), but future detailed bathymetric analysis is needed to further evaluate this.

3.2 Region-specific complexities during unzipping

We argue that the lithospheric unzipper concept explains the shared characteristics of the three cases that we discussed in this paper, but each also has region-specific additional complexities. We will discuss here how and whether they may be reconciled with the unzipper hypothesis, and whether it provides a better explanation than previous interpretations.

The lack of high-pressure metamorphism and the Barrovian conditions in the Menderes Massif shortly after underthrusting were previously explained by delamination, whereby the lithosphere would have gradually peeled back from north to south (van Hinsbergen et al., 2010), as in the numerical models of Göğüş & Pysklywec (2008) and Memiş et al. (2020). However, in that concept, low-angle, large-distance underthrusting should have involved the entire downgoing plate, requiring flat slab advance and subsequent rollback of the mantle lithosphere. This hypothesis has difficulty explaining why in Eocene and Oligocene time, shortly after accretion of the nappes, there was arc magmatism only tens of kms north of the Menderes massif. Moreover, the gradual peeling back of lithosphere is a process in which there is no plate boundary, and without net plate convergence (Göğüş & Ueda, 2018b; McPhee et al., 2019), whereas Africa-Europe convergence has been continuous. With the lithospheric unzipper hypothesis, subduction may have continued with a single, mantle-stationary or slowly retreating slab during accretion such that arc-trench distances remained stable, and the unzipped crust was underthrust far below the accretionary orogen in the upper plate (Figure 4). In western Anatolia, this underthrusting continued until all continental lithosphere was consumed, after which oceanic subduction resumed, about 35 Ma ago (van Hinsbergen et al., 2010). Part of this unzipped crust never underthrusted the orogen but remained in the foreland as the Bey Dağları platform of southwestern Turkey (van Hinsbergen et al., 2010).

Previous hypotheses to explain the high-temperature metamorphism in the Kırşehir Massif suggested delamination or slab break-off as heat source (Ilbeyli & Kibici, 2009; Köksal et al., 2012). Alternatively, because the reconstructed trench orientation at which the the Kırşehir Massif was N-S and the angle of underthrusting was NNE-SSW, obliquity of subduction was postulated to cause elevated prograde geothermal gradients (van Hinsbergen et al., 2016). Later, numerical experiments showed that obliquity decreases burial rates and therefore allows for higher geothermal gradients during burial (Plunder et al., 2018). However, while these hypotheses may explain part of the observations, they do not explain why the Kırşehir Massif underthrusted ~150 km below the upper plate, followed within a few Ma by the intrusion of arc plutons, and with the upper plate in extension during underthrusting.

The unzipper straightforwardly explains the large distance of underthrusting of the Kırşehir Block, towards the position of the arc by 85 Ma, by which time the block had already undergone Barrovian metamorphism and pervasive shearing (Figure 5). Because the Kırşehir block would have remained connected to the downgoing slab during underthrusting, its underthrusting direction was NNE-SSW consistent with syn-metamorphic stretching lineations (Lefebvre, 2011; van Hinsbergen et al., 2016). Upper plate extension, instead, both in the ophiolites (van Hinsbergen et al., 2016), as well as post-accretionary extension that exhumed the Kırşehir massif and surrounding metamorphic massifs (Gürer et al., 2018; Lefebvre et al., 2013) was E-W directed, i.e. at high angles to the subduction direction but perpendicular to the slab that rolled back westwards (Maffione et al., 2017; van Hinsbergen et al., 2020). These two deformation directions reflect the difference between relative plate convergence, and the relative motion between the trench that here was retreating from the overriding plate (Figure 5).

Finally, the complexity of the Oligocene-early Miocene of the Aegean region is that the HP-LT metamorphism of the PQ-Plattenkalk tandem occurs simultaneously with, and to the south of the Barrovian metamorphism of the Naxos-Samos Basal Unit. This requires that the two units underthrusted synchronously, the Barrovian Naxos-Samos Basal Unit north, and in front of, the PQ and Plattenkalk units (Figure 6). A previous explanation for this contrast invoked that the underthrusting of the Naxos-Paros-Samos Basal Unit occurred around the same time as the Cycladic Blueschist Unit, after which slab break-off occurred, the Naxos Basal Unit gradually heated up due to crustal thickening, and that renewed subduction to the south caused the formation of the Phyllite-Quartzite unit (Searle & Lamont, 2020). However, seismic tomographic images of the slab below the Aegean region give no reason to infer more than one subducted slab was formed during Aegean orogenesis (van Hinsbergen et al., 2005a); stratigraphic data show that the Basal Unit correlates to the Tripolitza unit that had the PQ represents the Tripolitza's stratigraphic underpinnings; and that these collectively underthrusted in Oligocene to earliest Miocene time, i.e. long after the underthrusting of the Cycladic Blueschist unit (Schmid et al., 2020). Moreover, geochronological data show that the Basal Unit and PQ reached peak metamorphic conditions (except for younger overprints around granitoids) simultaneously, around 20 Ma (Jolivet et al., 2010a; Lamont et al., 2020a; 2023b). Hence, we envisage that the underthrusting of the Basal Unit and the PQ/Plattenkalk tandem occurred simultaneously and in-sequence (Figure 6).

Based on the structural and stratigraphic evidence for simultaneous underthrusting of the Tripolitza and Ionian nappes from the western Hellenic foreland (Sotiropoulos et al., 2003; van Hinsbergen & Schmid, 2012), we postulate that the unzipping of the Tripolitza Platform/Basal Unit crust occurred while the platform was for a large part still in a foreland basin position, similarly to the Bey Dağları platform of southwest Turkey (Figure 1). The unzipped Tripolitza crust/Basal Unit underthrusted the orogen at low angle, while the Ionian Zone dipped steeper into the mantle. We tentatively infer that the thrust that buried the Ionian Zone stepped up through the stratigraphy below the adjacent Tripolita Platform, such that the PQ stratigraphic underpinnings of the Tripolitza Platform were buried as part of the Ionian nappe (Figure 6). This thrust may have been reactivated as detachment to bring the Phyllite Quarzite Unit back against the Tripolitza Platform carbonates on the Peloponnesos and Crete, during the burial of the more external parts of the Ionian zone that are preserved as the Plattenkalk Unit. With this regional modification the unzipper hypothesis may thus explain how two nappes simultaneously formed in sequence, in the same orogen, under contrasting metamorphic conditions, and during roll-back that extended the upper plate (Figure 6).

3.3 Nappe accretion versus unzipping versus slab break-off

From the examples above suggest a first-order relationship between the thickness of the subducting continental crust and the style of accretion. It has been well-established that between the ‘default’ modes of, on the one hand, wholesale subduction of oceanic lithosphere and, in the other hand, arrest of subduction upon the arrival of thick, unextended continental lithosphere, there is a mode of subduction of thinned continental crust that is facilitated by the accretion of its buoyant upper crust (Capitanio et al., 2010; Toussaint et al., 2004). This mode is reflected by thin-skinned nappe stacking and associated HP-LT metamorphism (Jolivet et al., 2003; van Hinsbergen et al., 2005). The ‘unzipper’ hypothesis adds another step that may be imaged as a downward stepping decollement horizon with an increasing continental crustal thickness (Figure 7). Based on our observations that the unzipped crust was overlain by shallow-water sediments, whereas thin-skinned HP-LT nappes contain deep-marine sediments, we infer that the unzipping occurs when thicker continental crust arrives in the trench, as a step between thin-skinned nappe accretion and the arrest of continental subduction altogether.

Recently, Liu et al. (2023) may have caught the process of downgoing continental lithosphere ‘unzipping’ in the act in the eastern Indian continent that is underthrusting below the easternmost Himalaya. These authors showed seismological evidence that a wedge of asthenosphere may be present between the horizontally underthrusting Indian crust below eastern Tibet, and steeper-plunging mantle lithospheric parts. Moreover, they show tha in regions above where this horizontal tear is imaged, hot springs release Helium with compositions consistent with the presence of asthenosphere at shallow depth. These recent results provide independent confirmation for the process of unzipping that we interpreted from the geological record. The results of Liu et al. (2023) are from the easternmost Indian continent, underthrusted below Tibet, that formed the conjugate margin to SW Australia (van Hinsbergen et al., 2019). This was likely extended and thinner than the thicker cratonic India to the west, and thus more prone to unzipping than to abrupt slab break-off that occurred along the rest of the Indian continental margin (Replumaz et al., 2010; van Hinsbergen, 2022; Webb et al., 2017) (Figure 7).

3.4 Unzipping elsewhere and on the Proterozoic Earth?

The metamorphic contrasts that we summarized from the eastern Mediterranean region are not unique. For instance, be the Eocene high-temperature metamorphism and anatexis that occurred in rocks of the Greater Himalaya crystallines that are traced over ~1500 km of the Himalayan orogen underwent prograde HT/MP (730-775°C / 10-13 kbar (Corrie & Kohn, 2011; Khanal et al., 2021). This metamorphism started around 50 Ma and continuing throughout the Eocene (Khanal et al., 2021; Smit et al., 2014), escaped HP-LT metamorphism (Stübner et al., 2014) and underwent partial melting developing leucogranites within ~10 Ma after their incorporation in the Himalayan orogen (e.g., Cao et al., 2022). In the far northwest of the Himalaya, rocks of the northwestern Greater Indian continental margin underwent UHP-LT (22-23 kbar, 400-425°C) instead, with metamorphism starting 57 Ma and HP/LT conditions prevailing until ~47 Ma onwards (Chatterjee & Jagoutz, 2015; de Sigoyer et al., 2000; Guillot et al., 2008; Leech et al., 2005; Palin et al., 2017), i.e. simultaneously with the HT/MP conditions along the Greater Himalayan rocks to the east. Bird (1978) already suggested that the HT conditions in the Greater Himalaya may be explained by delamination of the Indian Plate during underthrusting – equivalent to our unzipper hypothesis. Combined with the (U)HP-LT metamorphism of the Tso Morari complex in the far northwestern corner of the Tethyan Himalaya, this pair may be equivalent to, albeit a larger scale, Menderes and Cycladic Blueschist contrast (Figure 4).

The lithospheric unzipper hypothesis may also explain Barrovian conditions in the deep parts of accretionary Phanerozoic orogens elsewhere. For instance, we postulate that the rapid Barrovian conditions reached by the Venidigner Nappe in the heart of the Tauern Window may record the unzipping of downgoing Eurasian lithosphere. The Venidigner Nappe is the deepest, youngest nappe of the eastern Alps, not only contains sedimentary cover units but also underlying Paleozoic basement of the Eurasian Variscan belt, escaped HP-LT metamorphism, but is overlain by thin-skinned thrust slices that recorded a protracted history of HP-LT metamorphism (Smye et al., 2011; Schmid et al., 2013). In both the Alps and Himalaya, the architecture and sequence of tectonic and metamorphic events bear resemblance that of the eastern Mediterranean examples and may potentially be explained by the unzipping hypothesis.

Previous concepts of nappe accretion and associated HP-LT metamorphism reconciled the apparent jumps in subduction thrusts in geological records of orogens that appear as jumping subduction zones with the activity of a single subduction zone that consumed oceanic and continental lithosphere (Handy et al., 2010; Jolivet & Brun, 2010; Tirel et al., 2013; van Hinsbergen et al., 2005a). This satisfied the geophysical observations that show a continuous slab at depth below these orogens. The unzipper hypothesis may now also reconcile the presence of hot Barrovian continental units in those orogens that escaped HP-LT metamorphism with a continuous process of shallow angle (continental) subduction.

This may offer a geodynamic scenario that could explain the formation of hot Proterozoic orogens in context of subduction. For instance, the Paleoproterozoic Trans-Hudson orogen of North-America (Figure 8), a deeply eroded accretionary orogen (Corrigan et al., 2009), is characterized by the abundance of accreted, thick continental crystalline basement with only rare supracrustal nappes. These units do not reveal evidence of early orogenic HP-UHP metamorphism but display predominantly Barrovian metamorphism that commonly reaches granulites facies temperatures but rarely reaches pressures above 8-10 kbar. These conditions overlap with or predating arc magmatism, and even though the continental fragments that constitute the orogen have markedly different geological histories and are interpreted to represent individual microcontinent, there is a near total absence of ophiolites or oceanic material between these accreted terranes (Corrigan et al., 2009; Godet et al., 2021; St-Onge et al., 2006; Weller et al., 2013, and references therein). More specifically, the South-East Churchill Province branch (Corrigan et al., 2018; Godet et al., 2021; Wardle et al., 2002) of the Trans-Hudson Orogen (Figure 8) is comprised of upper amphibolite to granulite facies crystalline basement units of 50-100 km wide, the Core Zone, separating the lower plate Superior craton and its rifted margin volcanic-sedimentary sequences (the Labrador Trough) from the upper plate North Atlantic Craton (Figure 8). Arc magmatism swept across the core zone from the upper plate towards the lower plate, always predated by Barrovian metamorphism (Godet et al., 2021). Maximum pressures recorded were on the order of 11 kbar for granulite facies rocks (Charette et al., 2021; Godet et al., 2021), with a preserved Barrovian sequence on the western edge of the orogen (Godet et al., 2020).

Several long-lived crustal-scale anastomosing shear zones within the Core Zone separate continental blocks of contrasting isotopic signatures, leading authors to interpret them as microcontinents with each shear zone representing individual suture zones (Corrigan et al., 2018; 2021), i.e. former subduction zones that must have consumed oceanic lithosphere by wholesale subduction, leading to an absence of oceanic exotic material in between the continental fragments. The sweeping of arc magmatism is thus implicitly seen as individual arcs birthing and dying as small ocean basins sequentially subduct and close between the terranes, with separate subduction initiation events within each basin, and multiple slabs involved (e.g., Corrigan et al., 2018; 2021; Wardle et al., 2002). However, Godet et al. (2021), in their regional magmatic and metamorphic compilation, already noted that the orogenic architecture is not as expected for a modern accretionary orogen that formed in such a fashion such as Mesozoic-Cenozoic Tibet (Kapp & DeCelles, 2019), noting the absence of oceanic material or (U)HP-LT metamorphism, and the rapid development and duration of granulite conditions directly after accretion and even before the arrival of arc magmatism. We propose that such characteristics may be well explained by successive accretion of pericratonic microcontinents through lithospheric unzipping (Figure 8). Such an explanation requires only one eastward-dipping slab (present-day coordinates) that subducted over the 150 Myrs evolution of the South-East Churchill Province, as previously postulated by Godet (2020). We postulate that the decollement horizon coincided with the top of the crust in the oceanic basins and stepped down to the Moho in the intervening microcontinents. This then led to successive accretion through lithospheric unzipping of Superior affinity peri-cratonic blocks to the North Atlantic Craton accompanied by slab roll-back relative to that craton left the upper plate without a thick lithospheric mantle, providing an explanation for the widespread lower-plate-ward sweeping of granulite facies metamorphic conditions closely followed by arc magmatism, and for penetrative deformation and coeval anastomosed shear zone development all throughout the Province.

If in a hotter Earth, the Moho was weaker and more prone to becoming the decollement horizon than the sediment-basement interface, lithospheric unzipping may have been the rule rather than the exception. This mode of orogenesis may have been the default until continents became strong enough so that their thinned margins became dragged down into subduction zones. This transition may have occurred at around 650 Ma, when metamorphic, geochemical, and plate tectonic lines of evidence suggest that deep continental recycling into the mantle initiated (Brown & Johnson, 2018; Brown et al., 2022; Jackson & Macdonald, 2022). The lithospheric unzipper concept may thus explain hot Proterozoic orogenesis as a geological expression of modern-style (continental) subduction in an Earth that was much hotter than today.

3. Conclusions

Phanerozoic accretionary orogens typically consist of thin-skinned, upper crustal nappes that were offscraped from subducted oceanic or continental lithosphere that, where sufficiently buried, display (ultra) high-pressure, low-temperature (U)HP-LT metamorphism. These are straightforwardly explained by the progressive, episodic decoupling of upper crustal units during ongoing subduction, whereby the typical cold metamorphism is explained by burial and exhumation of nappes along the plate interface. Surprisingly, however, the deepest continental structural units of accretionary mountain belts often escaped HP-LT metamorphism and underwent prograde, ‘Barrovian’ MP-HT metamorphism instead. Here we review three of these enigmatic Barrovian complexes in the eastern Mediterranean region and compare each of these to time-equivalent HP-LT metamorphic nappes that formed laterally at the same subduction zone. These include the Barrovian Kırşehir Block, Menderes Massif, and Naxos-Samos Basal Unit, which formed simultaneously with the HP-LT metamorphic Tavşanlı zone, Cycladic Blueschist, and Phyllite-Quartzite/Plattenkalk units. We conclude that the continental units that underwent prograde Barrovian metamorphism underthrusted at low angle below the forearc over distances of up to 150 km or more, likely still contain the entire pre-orogenic continental crust but not their mantle lithosphere, and reached close to or even beyond the location of the magmatic arc that intruded the unit after accretion. We postulate that this major horizontal underthrusting is the result of a process of gradual ‘unzipping’ of the low-angle underthrusting crust from the steeply subducting Moho. The underthrusting crust penetrates between the upper plate lithosphere and the underlying mantle wedge and, unprotected by its decoupled and subducting mantle lithospheric underpinnings, undergo high-temperature metamorphism and pervasive shearing. The process of lithospheric unzipping in the eastern Mediterranean orogens likely forms an intermediate stage between steep continental margin subduction and thin-skinned nappe accretion, and the arrest of subduction upon arrival of thick, unstretched continent. We postulate that in a hotter, Proterozoic Earth, the process of unzipping may have been the default response of continents to subduction, making enigmatic hot orogenesis characteristics for Proterozoic orogens, such as in the Trans-Hudson orogen of Canada, possible geological expressions of modern-style continental subduction in a hotter Earth.

Acknowledgements

DJJvH acknowledges NWO Vici grant 865.17.001. CG acknowledges NSERC funding (grant RGPIN-2020-06400).

Open Research

No new codes or data were used for this paper: these are available through the cited references.

Figure 1: A) Tectonic map of the Aegean and Anatolian regions, with the modern and restored positions of the synchronous nappes with contrasting thermal evolutions. B, C, D) Paleo-tectonic reconstructions, based on van Hinsbergen et al. (2020), showing the paleogeographic positions during underthrusting of the Phyllite-Quartzite/Plattenkalk vs. Basal Unit, Cyclading Blueschist Unit versus Menderes Massif, and the Tavşanlı Zone vs Kırşehir Block, respectively. AZ = Afyon Zone; BD = Bey Dağları platform; CAO = Central Anatolian Ophiolites; CBU = Cycladic Blueschist Unit; Io = Ionian Nappe; KB = Kırşehir Block; LN = Lycian Nappes; MB = Mesohellenic Basin; MM = Menderes Massif; NAFZ = North Anatolian Fault Zone; NBU = Naxos Basal Unit; Pi = Pindos Nappe; PQ/PK = Phyllite-Quartzite/Plattenkalk units; SaS =. Sava Suture Zone; Tr = Tripolitza Nappe; TZ = Tavşanlı Zone. B, C, D) Tectonic reconstructions at 20, 45, and 85 Ma, corresponding to the timing of underthrusting of the Phyllite-Quartzite/Plattenkalk and Basal Unit, Cyclading Blueschist Unit and Menderes Massif, and Tavşanlı Zone and Kırşehir Block, respectively. E, F, G) lithospheric cross-sections across the Aegean, west Anatolian, and central Anatolian orogenic segments, respectively. Sections A-A' is modified from Schmid et al. (2020): those authors presumed that the crust underlying all of the Aegean orogen from the Sava Suture Zone to the south was underlain by Ionian Nappe continental crust. The steep subduction of the Phlyllite-Quartzite/Plattenkalk units found in the Aegean forearc of Crete and the Peloponnesos precludes this, and instead, we here interpret the Aegean crust north of Crete to be underlain by Naxos Basal Unit/Tripolitza crust. Section B-B' is modified from van Hinsbergen et al. (2010) and Schmid et al. (2020). Section C-C' is modified from van McPhee et al. (2022).

Figure 2: Compilation of P-T-t paths and estimates of peak metamorphic conditions for HP-LT nappes and MP-HT nappes for the three case study areas. HP-LT nappes include: the Tavsanli Zone (green), 24 kbar, 500°C (Davis & Whitney, 2008; Okay, 2002; Plunder et al., 2013). Lu/Hf geochronology on garnet and lawsonite between ~91-83 Ma (Mulcahy et al., 2014; Pourteau et al., 2019). Cycladic Blueschist Unit (dark blue), 18-23 kbar, 500-600°C and U/Pb zircon and allanite and Lu/Hf garnet ages between ~55-38 Ma (Behr et al., 2018; Lamont et al., 2020c; Laurent et al., 2017; Skelton et al., 2019; Wolfe et al., 2023). Phyllite Quartzite Unit (light blue) 18 kbar 400°C dated at ~24-20 Ma by Ar-Ar (Jolivet et al., 1996;

2010b). MP-HT nappes that are coeval with HP-LT nappes include: the Kırşehir Massif (orange) 5-8 kbar, 700°C (Lefebvre et al., 2015; Whitney & Dilek, 1998; Whitney & Hamilton, 2004; Whitney et al., 2003), dated at ~90-85 Ma by U-Pb monazite and zircon (Whitney & Hamilton, 2004; Whitney et al., 2003). Menderes Massif (yellow) 6-8 kbar and 500-550°C (Okay, 2001; Whitney & Bozkurt, 2002), at ~42 and 35 Ma dated by Lu/Hf on garnet (Schmidt et al., 2015), Rb-Sr (Bozkurt et al., 2011) and 40Ar-39Ar syn-metamorphic ages of greenschists (Lips et al., 2001). Naxos Basal Unit (red) ~10-11 kbar and ~600-730°C, dated by U-Pb zircon at 20-16 Ma (Keay & Lister, 2002; Lamont et al., 2020b; 2023b)

Figure 3: The lithospheric unzipper concept versus deep underthrusting and nappe stacking. During lithospheric unzippin, the decollement steps down from to Moho depths, and the buoyant downgoing plate's crust underthrusts the upper plate at low angle while the mantle lithosphere subducts steeply.

Figure 4. 3D cartoon showing the contrasting deep subduction and nappe stacking of the Cycladic Blueschist Unit versus lithospheric unzipping and low-angle underthrusting of the Menderes Massif.

Figure 5. 3D cartoon showing the contrasting deep subduction and nappe stacking of the Tavşanlı zone, versus lithospheric unzipping and low-angle underthrusting of the Kırşehir Block at nearly perpendicular trenches.

Figure 6. 2D cross sections showing the simultaneous underthrusting of the unzipped, low-angle underthrusting Basal Unit and the steeply subducting Phyllite-Quartzite and Plattenkalk units. These processes occurred during roll-back, below an extending upper plate.

Figure 7. Four stages of subduction as a function of the down-stepping of a decollement through a continental lithosphere, from whole-sale subduction, to nappe stacking, to unzipping, to slab break-off.

Figure 8. A) Tectonic map of the Trans-Hudson orogen and the South-East Churchill province, modified after Corrigan et al. (2021); B) Cross-section of the accreted continental crustal fragments of the Core Zone of the South-East Churchill Province modified after Corrigan et al. (2021); C) schematic diagram illustrating the decollement location in a conceptual pre-orogenic cross section. If the decollement horizon coincided with the Moho of the microcontinental fragments such that they unzipped during continental subduction, and with the top of the crust of intervening oceanic basins, the juxtaposition of the continents without intervening accretionary prisms, and their westward sweeping Barrovian metamorphism trailed by arc magmatism may be explained by the continuous subduction of a single slab. See text for further discussion.

4. References

Abgarmi, B., Delph, J. R., Ozacar, A. A., Beck, S. L., Zandt, G., Sandvol, E., et al. (2017). Structure of the crust and African slab beneath the central Anatolian plateau from receiver functions: New insights on isostatic compensation and slab dynamics. *Geosphere, 13*(6), 1774-1787.

Advokaat, E. L., van Hinsbergen, D. J. J., Kaymakcı, N., Vissers, R. L. M., & Hendriks, B. W. H. (2014). Late Cretaceous extension and Palaeogene rotation-related contraction in Central Anatolia recorded in the Ayhan-Büyükkışla basin. *International Geology Review, 56*(15), 1813-1836.

Akay, E. (2009). Geology and petrology of the Simav Magmatic Complex (NW Anatolia) and its comparison with the Oligo-Miocene granitoids in NW Anatolia: implications on Tertiary tectonic evolution of the region. *International Journal of Earth Sciences, 98*, 1655-1675.

Altherr, R., Henjes-Kunst, F., Matthews, A., Friedrichsen, H., & Hansen, B. T. (1988). O-Sr istotopic variations in Miocene granitoids from the Aegean: Evidence for an origin by combined assimilation and fractional crystallisation. *Contributions to Mineralogy and Petrology, 100*, 528-541.

Barazangi, M., Sandvol, E., & Seber, D. (2006). Structure and tectonic evolution of the Anatolian plateau in eastern Turkey. *Geological Society of America Special Paper, 409*, 463-473.

Behr, W. M., Kotowski, A. J., & Ashley, K. T. (2018). Dehydration-induced rheological heterogeneity and the deep tremor source in warm subduction zones. *Geology, 46*(5), 475-478.

Berk Biryol, C., Beck, S. L., Zandt, G., & Özacar, A. A. (2011). Segmented African lithosphere beneath the Anatolian region inferred from teleseismic P-wave tomography. *Geophysical Journal International, 184*(3), 1037-1057.

Bird, P. (1978). Initiation of intracontinental subduction in the Himalaya. *Journal of Geophysical Research: Solid Earth*, *83(B10)*, 4975-4987.

Blumor, T., Dollinger, J., Mutter, A., Zardam, S., & Kowalczyk, G. (1994). Plattenkalk Series and kastania Phyllites of the Taygetos MTS.: new results on structure and succession. *Δελτίον της Ελληνικής Γεωλογικής Εταιρίας, 30*(2), 83-92.

Bozkurt, E., & Oberhänsli, R. (2001). Menderes Massif (Western Turkey): structural, metamorphic and magmatic evolution - a synthesis. *International Journal of Earth Sciences, 89*(4), 679-708.

Bozkurt, E., Satır, M., & Buğdaycıoğlu, Ç. (2011). Surprisingly young Rb/Sr ages from the Simav extensional detachment fault zone, northern Menderes Massif, Turkey. *Journal of Geodynamics, 52*(5), 406-431.

Bröcker, M., & Pidgeon, R. T. (2007). Protolith ages of meta-igneous and metatuffaceous rocks from the Cycladic blueschist unit, Greece: results of a reconnaissance U-Pb zircon study. *The Journal of Geology, 115*(1), 83-98.

Brown, M. (1993). P–T–t evolution of orogenic belts and the causes of regional metamorphism. *Journal of the Geological Society, 150*(2), 227-241.

Brown, M. (2007). Metamorphic conditions in orogenic belts: a record of secular change. *International Geology Review, 49*(3), 193-234.

Brown, M., & Johnson, T. (2018). Secular change in metamorphism and the onset of global plate tectonics. *American Mineralogist, 103*(2), 181-196.

Brown, M., Johnson, T., & Spencer, C. J. (2022). Secular changes in metamorphism and metamorphic cooling rates track the evolving plate-tectonic regime on Earth. *Journal of the Geological Society, 179*(5), jgs2022-2050.

Brun, J.-P., & Faccenna, C. (2008). Exhumation of high-pressure rocks driven by slab rollback. *Earth and Planetary Science Letters, 272*(1-2), 1-7.

Brun, J.-P., & Sokoutis, D. (2007). Kinematics of the Southern Rhodope Core Complex (North Greece). *International Journal of Earth Sciences, 96*(6), 1079-1099.

Brun, J. P., & Sokoutis, D. (2010). 45 m.y. of Aegean crust and mantle flow driven by trench retreat. *Geology, 38*(9), 815-818.

Candan, O., Çetinkaplan, M., Oberhänsli, R., Rimmelé, G., & Akal, C. (2005). Alpine high-P/low-T metamorphism of the Afyon Zone and implications for the metamorphic evolution of Western Anatolia, Turkey. *Lithos, 84*(1-2), 102-124.

Cao, H.-W., Pei, Q.-M., Santosh, M., Li, G.-M., Zhang, L.-K., Zhang, X.-F., Zhang, Y.-H., Zou, H., Dai, Z.-W. and Lin, B. (2022). Himalayan leucogranites: A review of geochemical and isotopic characteristics, timing of formation, genesis, and rare metal mineralization, *Earth-Science Reviews, 104229.*

Capitanio, F. A., Morra, G., Goes, S., Weinberg, R. F., & Moresi, L. (2010). India–Asia convergence driven by the subduction of the Greater Indian continent. *Nature Geoscience, 3*(2), 136-139.

Cawood, P. A., Kröner, A., Collins, W. J., Kusky, T. M., Mooney, W. D., & Windley, B. F. (2009). Accretionary orogens through Earth history. *Geological Society, London, Special Publications, 318*(1), 1-36.

Charette, B., Godet, A., Guilmette, C., Davis, D. W., Vervoort, J., Kendall, B., et al. (2021). Long-lived anatexis in the exhumed middle crust of the Torngat Orogen: Constraints from phase equilibria modeling and garnet, zircon, and monazite geochronology. *Lithos, 388*, 106022.

Chatterjee, N., & Jagoutz, O. (2015). Exhumation of the UHP Tso Morari eclogite as a diapir rising through the mantle wedge. *Contributions to Mineralogy and Petrology, 169*, 1-20.

Cisneros, M., Barnes, J. D., Behr, W. M., Kotowski, A. J., Stockli, D. F., & Soukis, K. (2021). Insights from elastic thermobarometry into exhumation of high-pressure metamorphic rocks from Syros, Greece. *Solid Earth, 12*(6), 1335-1355.

Collins, A. S., & Robertson, A. H. F. (2003). Kinematic evidence for Late Mesozoic–Miocene emplacement of the Lycian Allochthon over the western Anatolide belt, SW Turkey. *Geological Journal, 38*(3-4), 295-310.

Corrie, S. L., & Kohn, M. J. (2011). Metamorphic history of the central Himalaya, Annapurna region, Nepal, and implications for tectonic models. *Bulletin, 123*(9-10), 1863-1879.

Corrigan, D., Pehrsson, S., Wodicka, N., & De Kemp, E. (2009). The Palaeoproterozoic Trans-Hudson Orogen: a prototype of modern accretionary processes. *Geological Society, London, Special Publications, 327*(1), 457-479.

Corrigan, D., van Rooyen, D., & Wodicka, N. (2021). Indenter tectonics in the Canadian Shield: A case study for Paleoproterozoic lower crust exhumation, orocline development, and lateral extrusion. *Precambrian Research, 355*, 106083.

Corrigan, D., Wodicka, N., McFarlane, C., Lafrance, I., Rooyen, D. v., Bandyayera, D., & Bilodeau, C. (2018). Lithotectonic framework of the core zone, Southeastern Churchill Province, Canada. *Geoscience Canada, 45*(1), 1-24.

Cossette, É., Audet, P., Schneider, D., & Grasemann, B. (2016). Structure and anisotropy of the crust in the Cyclades, Greece, using receiver functions constrained by in situ rock textural data. *Journal of Geophysical Research: Solid Earth, 121*(4), 2661-2678.
Davis, P. B., & Whitney, D. L. (2008). Petrogenesis and structural petrology of high-pressure metabasalt pods, Sivrihisar, Turkey. *Contributions to Mineralogy and Petrology, 156*(2), 217-241.
de Sigoyer, J., Chavagnac, V., Blichert-Toft, J., Villa, I. M., Luais, B., Guillot, S., et al. (2000). Dating the Indian continental subduction and collisional thickening in the northwest Himalaya: Multichronology of the Tso Morari eclogites. *Geology, 28*(6), 487-490.
Dragovic, B., Samanta, L. M., Baxter, E. F., & Selverstone, J. (2012). Using garnet to constrain the duration and rate of water-releasing metamorphic reactions during subduction: An example from Sifnos, Greece. *Chemical Geology, 314*, 9-22.
Endrun, B., Lebedev, S., Meier, T., Tirel, C., & Friederich, W. (2011). Complex layered deformation within the Aegean crust and mantle revealed by seismic anisotropy. *Nature Geoscience, 4*(3), 203-207.
England, P. C., & Thompson, A. B. (1984). Pressure—temperature—time paths of regional metamorphism I. Heat transfer during the evolution of regions of thickened continental crust. *Journal of Petrology, 25*(4), 894-928.
Ersoy, E. Y., & Palmer, M. R. (2013). Eocene-Quaternary magmatic activity in the Aegean: Implications for mantle metasomatism and magma genesis in an evolving orogeny. *Lithos, 180*, 5-24.
Fassoulas, C., Kilias, A., & Mountrakis, D. (1994). Postnappe stacking extension and exhumation of high-pressure/low-temperature rocks in the island of Crete, Greece. *Tectonics, 13*, 127-138.
Floyd, P. A., Göncüoğlu, M. C., Winchester, J. A., & Yaliniz, M. K. (2000). Geochemical Character and Tectonic Environment of Neotethyan Ophiolitic Fragments and Metabasites in the Central Anatolian Crystalline Complex, Turkey. *Geological Society, London, Special Publications, 173*(1), 183-202.
Gessner, K., Ring, U., & Güngör, T. (2011). Field Guide to Samos and the Menderes Massif: Along-Strike Variations in the Mediterranean Tethyan Orogen. *Geological Society of America Field Guide, 23*, 1-52.
Gessner, K., Ring, U., Passchier, C. W., & GÜNGÖR, T. (2001). How to resist subduction: evidence for large-scale out-of-sequence thrusting during Eocene collision in western Turkey. *Journal of the Geological Society, 158*(5), 769-784.
Godet, A. (2020). Styles métamorphique et tectonique au Paléoprotérozoïque: Exemple du sud-est de la province du Churchill, Québec, Canada. *PhD Thesis, Université Laval*, 396 pp.
Godet, A., Guilmette, C., Labrousse, L., Smit, M. A., Cutts, J. A., Davis, D. W., & Vanier, M. A. (2021). Lu–Hf garnet dating and the timing of collisions: Palaeoproterozoic accretionary tectonics revealed in the Southeastern Churchill Province, Trans-Hudson Orogen, Canada. *Journal of Metamorphic Geology, 39*(8), 977-1007.
Godet, A., Guilmette, C., Labrousse, L., Smit, M. A., Davis, D. W., Raimondo, T., et al. (2020). Contrasting PTt paths reveal a metamorphic discontinuity in the New Quebec Orogen: Insights into Paleoproterozoic orogenic processes. *Precambrian Research, 342*, 105675.
Göğüş, O. H., & Pysklywec, R. N. (2008). Mantle lithosphere delamination driving plateau uplift and synconvergent extension in eastern Anatolia. *Geology, 36*(9), 723-726.

Göğüş, O. H., Pysklywec, R. N., & Faccenna, C. (2016). Postcollisional lithospheric evolution of the Southeast Carpathians: Comparison of geodynamical models and observations. *Tectonics, 35*(5), 1205-1224.
Göğüş, O. H., & Ueda, K. (2018a). Peeling back the lithosphere: Controlling parameters, surface expressions and the future directions in delamination modeling. *Journal of Geodynamics, 117*, 21-40.
Göğüş, O. H., & Ueda, K. (2018b). Peeling back the lithosphere: Controlling parameters, surface expressions and the future directions in delamination modeling. *Journal of Geodynamics*.
Gorce, J. S., Caddick, M. J., Baxter, E. F., Dragovic, B., Schumacher, J. C., Bodnar, R. J., & Kendall, J. F. (2021). Insight into the early exhumation of the Cycladic Blueschist Unit, Syros, Greece: Combined application of zoned garnet geochronology, thermodynamic modeling, and quartz elastic barometry. *Geochemistry, Geophysics, Geosystems, 22*(8), e2021GC009716.
Guillot, S., Mahéo, G., de Sigoyer, J., Hattori, K. H., & Pêcher, A. (2008). Tethyan and Indian subduction viewed from the Himalayan high- to ultrahigh-pressure metamorphic rocks. *Tectonophysics, 451*(1-4), 225-241.
Gülyüz, E., Kaymakci, N., Meijers, M. J. M., van Hinsbergen, D. J. J., Lefebvre, C., Vissers, R. L. M., et al. (2013). Late Eocene evolution of the Çiçekdağı Basin (central Turkey): Syn-sedimentary compression during microcontinent–continent collision in central Anatolia. *Tectonophysics, 602*, 286-299.
Gürer, D., Plunder, A., Kirst, F., Corfu, F., Schmid, S. M., & van Hinsbergen, D. J. J. (2018). A long-lived Late Cretaceous–early Eocene extensional province in Anatolia? Structural evidence from the Ivriz Detachment, southern central Turkey. *Earth and Planetary Science Letters, 481*, 111-124.
Gürer, D., van Hinsbergen, D. J. J., Matenco, L., Corfu, F., & Cascella, A. (2016). Kinematics of a former oceanic plate of the Neotethys revealed by deformation in the Ulukışla basin (Turkey). *Tectonics, 35*(10), 2385-2416.
Hafkenscheid, E., Wortel, M. J. R., & Spakman, W. (2006). Subduction history of the Tethyan region derived from seismic tomography and tectonic reconstructions. *Journal of Geophysical Research, 111*(B8).
Handy, M. R., Schmid, S. M., Bousquet, R., Kissling, E., & Bernoulli, D. (2010). Reconciling plate-tectonic reconstructions of Alpine Tethys with the geological–geophysical record of spreading and subduction in the Alps. *Earth-Science Reviews, 102*(3-4), 121-158.
IGRS-IFP. (1966). Étude Géologique de l'Epire (Grèce Nord-occidentale). In: Technip Paris.
Ilbeyli, N. (2005). Mineralogical–geochemical constraints on intrusives in central Anatolia, Turkey: tectono-magmatic evolution and characteristics of mantle source. *Geological Magazine, 142*(2), 187-207.
Ilbeyli, N., & Kibici, Y. (2009). Collision-related granite magma genesis, potential sources and tectono-magmatic evolution: comparison between central, northwestern and western Anatolia (Turkey). *International Geology Review, 51*(3), 252-278.
Isik, V., Lo, C.-H., Göncüoğlu, C., & Demirel, S. (2008). 39Ar/40Ar Ages from the Yozgat Batholith: Preliminary Data on the Timing of Late Cretaceous Extension in the Central Anatolian Crystalline Complex, Turkey. *The Journal of Geology, 116*(5), 510-526.
Isik, V., Tekeli, O., & Seyitoglu, G. (2004). The 40Ar/39Ar age of extensional ductile deformation and granitoid intrusion in the northern Menderes core complex: implications for the initiation of extensional tectonics in western Turkey. *Journal of Asian Earth Sciences, 23*(4), 555-566.

Jackson, M., & Macdonald, F. (2022). Hemispheric geochemical dichotomy of the mantle is a legacy of austral supercontinent assembly and onset of deep continental crust subduction. *AGU Advances, 3*(6), e2022AV000664.
Jamieson, R. A., Beaumont, C., Fullsack, P., & Lee, B. (1998). Barrovian regional metamorphism: where's the heat? *Geological Society, London, Special Publications, 138*(1), 23-51.
Jamtveit, B., & Austrheim, H. (2010). Metamorphism: the role of fluids. *Elements, 6*(3), 153-158.
Jolivet, L., & Brun, J.-P. (2010). Cenozoic geodynamic evolution of the Aegean. *International Journal of Earth Sciences, 99*(1), 109-138.
Jolivet, L., Faccenna, C., Goffé, B., Burov, E., & Agard, P. (2003). Subduction tectonics and exhumation of high-pressure metamorphic rocks in the Mediterranean orogens. *American Journal of Science, 303*(5), 353-409.
Jolivet, L., Goffé, B., Monié, P., Truffert-Luxey, C., Patriat, M., & Bonneau, M. (1996). Miocene detachment in Crete and exhumation P-T-t paths of high-pressure metamorphic rocks. *Tectonics, 15*(6), 1129-1153.
Jolivet, L., Lecomte, E., Huet, B., Denèle, Y., Lacombe, O., Labrousse, L., et al. (2010). The North Cycladic Detachment System. *Earth and Planetary Science Letters, 289*(1-2), 87-104.
Jolivet, L., Menant, A., Sternai, P., Rabillard, A., Arbaret, L., Augier, R., et al. (2015). The geological signature of a slab tear below the Aegean. *Tectonophysics, 659*, 166-182.
Jolivet, L., Trotet, F., Monié, P., Vidal, O., Goffé, B., Labrousse, L., et al. (2010). Along-strike variations of P–T conditions in accretionary wedges and syn-orogenic extension, the HP–LT Phyllite–Quartzite Nappe in Crete and the Peloponnese. *Tectonophysics, 480*(1-4), 133-148.
Kapp, P., & DeCelles, P. G. (2019). Mesozoic–Cenozoic geological evolution of the Himalayan-Tibetan orogen and working tectonic hypotheses. *American Journal of Science, 319*(3), 159-254.
Kastens, K. A. (1991). Rate of outward growth of the Mediterranean Ridge accretionary complex. *Tectonophysics, 199*(1), 25-50.
Kaymakci, N., Özçelik, Y., White, S. H., & Van Dijk, P. M. (2009). Tectono-stratigraphy of the Çankırı Basin: Late Cretaceous to early Miocene evolution of the Neotethyan Suture Zone in Turkey. *Geological Society, London, Special Publications, 311*(1), 67-106.
Keay, S., & Lister, G. (2002). African provenance for the metasediments and metaigneous rocks of the Cyclades, Aegean Sea, Greece. *Geology, 30*(3), 235-238.
Khanal, G. P., Wang, J. M., Larson, K. P., Wu, F. Y., Rai, S. M., Wang, J. G., & Yang, L. (2021). Eocene metamorphism and anatexis in the Kathmandu Klippe, Central Nepal: implications for early crustal thickening and initial rise of the Himalaya. *Tectonics, 40*(4), e2020TC006532.
Koç, A., Kaymakci, N., Van Hinsbergen, D. J. J., & Kuiper, K. F. (2017). Miocene tectonic history of the Central Tauride intramontane basins, and the paleogeographic evolution of the Central Anatolian Plateau. *Global and Planetary Change, 158*, 83-102.
Köksal, S., Möller, A., Göncüoglu, M. C., Frei, D., & Gerdes, A. (2012). Crustal homogenization revealed by U–Pb zircon ages and Hf isotope evidence from the Late Cretaceous granitoids of the Agaçören intrusive suite (Central Anatolia/Turkey). *Contributions to Mineralogy and Petrology, 163*, 725-743.
Köksal, S., Romer, R. L., Göncüoglu, M. C., & Toksoy-Köksal, F. (2004). Timing of post-collisional H-type to A-type granitic magmatism: U–Pb titanite ages from the Alpine

central Anatolian granitoids (Turkey). *International Journal of Earth Sciences, 93*(6), 974-989.
Kotowski, A. J., & Behr, W. M. (2019). Length scales and types of heterogeneities along the deep subduction interface: Insights from exhumed rocks on Syros Island, Greece. *Geosphere, 15*(4), 1038-1065.
Kotowski, A. J., Cisneros, M., Behr, W. M., Stockli, D. F., Soukis, K., Barnes, J. D., & Ortega-Arroyo, D. (2022). Subduction, underplating, and return flow recorded in the Cycladic Blueschist Unit exposed on Syros, Greece. *Tectonics, 41*(6), e2020TC006528.
Krahl, J., Kauffmann, G., Kozur, H., Richter, D., Förster, O., & Heinritzi, F. (1983). Neue Daten zur biostratigraphie und zur tektonischen lagerung der Phyllit-Gruppe und der Trypali-Gruppe auf der Insel Kreta (Griechenland). *Geologische Rundschau, 72*(3), 1147-1166.
Lagos, M., Scherer, E. E., Tomaschek, F., Münker, C., Keiter, M., Berndt, J., & Ballhaus, C. (2007). High precision Lu–Hf geochronology of Eocene eclogite-facies rocks from Syros, Cyclades, Greece. *Chemical Geology, 243*(1-2), 16-35.
Lamont, T. N., Roberts, N. M., Searle, M. P., Gardiner, N. J., Gopon, P., Hsieh, Y.-T., et al. (2023a). Contemporaneous crust-derived I-and S-type granite magmatism and normal faulting on Tinos, Delos, and Naxos, Greece: Constraints on Aegean orogenic collapse. *Geological Society of America Bulletin*.
Lamont, T. N., Roberts, N. M., Searle, M. P., Gopon, P., Waters, D. J., & Millar, I. (2020a). The age, origin, and emplacement of the Tsiknias Ophiolite, Tinos, Greece. *Tectonics, 39*(1), e2019TC005677.
Lamont, T. N., Searle, M. P., Gopon, P., Roberts, N. M., Wade, J., Palin, R. M., & Waters, D. J. (2020b). The Cycladic Blueschist Unit on Tinos, Greece: Cold NE subduction and SW directed extrusion of the Cycladic continental margin under the Tsiknias Ophiolite. *Tectonics, 39*(9), e2019TC005890.
Lamont, T. N., Searle, M. P., Waters, D. J., Roberts, N. M., Palin, R. M., Smye, A., et al. (2020c). Constraints on the thermal evolution of metamorphic core complexes from the timing of high-pressure metamorphism on Naxos, Greece. *GSA Bulletin, 132*(1-2), 149-197.
Lamont, T. N., Smye, A. J., Roberts, N. M., Searle, M. P., Waters, D. J., & White, R. W. (2023b). Constraints on the thermal evolution of metamorphic core complexes from the timing of high-pressure metamorphism on Naxos, Greece. *Geological Society of America Bulletin*.
Laurent, V., Huet, B., Labrousse, L., Jolivet, L., Monie, P., & Augier, R. (2017). Extraneous argon in high-pressure metamorphic rocks: Distribution, origin and transport in the Cycladic Blueschist Unit (Greece). *Lithos, 272*, 315-335.
Leech, M., Singh, S., Jain, A., Klemperer, S., & Manickavasagam, R. (2005). The onset of India–Asia continental collision: Early, steep subduction required by the timing of UHP metamorphism in the western Himalaya. *Earth and Planetary Science Letters, 234*(1-2), 83-97.
Lefebvre, C. (2011). *The tectonics of the Central Anatolian Crystalline Complex: a structural, metamorphic and paleomagnetic study (PhD thesis)* (Vol. 3).
Lefebvre, C., Barnhoorn, A., van Hinsbergen, D. J. J., Kaymakci, N., & Vissers, R. L. M. (2011). Late Cretaceous extensional denudation along a marble detachment fault zone in the Kırşehir massif near Kaman, central Turkey. *Journal of Structural Geology, 33*(8), 1220-1236.
Lefebvre, C., Meijers, M. J. M., Kaymakci, N., Peynircioğlu, A., Langereis, C. G., & van Hinsbergen, D. J. J. (2013). Reconstructing the geometry of central Anatolia during

the late Cretaceous: Large-scale Cenozoic rotations and deformation between the Pontides and Taurides. *Earth and Planetary Science Letters, 366*, 83-98.

Lefebvre, C., Peters, M. K., Wehrens, P. C., Brouwer, F. M., & van Roermund, H. L. M. (2015). Thermal history and extensional exhumation of a high-temperature crystalline complex (Hırkadağ Massif, Central Anatolia). *Lithos, 238*, 156-173. http://www.sciencedirect.com/science/article/pii/S0024493715003424

Lips, A. L. W., Cassard, D., Sözbilir, H., Yilmaz, H., & Wijbrans, J. R. (2001). Multistage exhumation of the Menderes Massif, western Anatolia (Turkey). *International Journal of Earth Sciences, 89*(4), 781-792.

Liu, L., Shi, D., Klemperer, S. L., & Shi, J. (2023). Slab tearing and delamination of the Indian lithospheric mantle during flat-slab subduction, southeast Tibet. *Authorea Preprints*.

Maffione, M., van Hinsbergen, D. J. J., de Gelder, G. I. N. O., van der Goes, F. C., & Morris, A. (2017). Kinematics of Late Cretaceous subduction initiation in the Neo-Tethys Ocean reconstructed from ophiolites of Turkey, Cyprus, and Syria. *Journal of Geophysical Research: Solid Earth, 122*(5), 3953-3976.

Marsellos, A. E., Kidd, W. S. F., & Garver, J. I. (2010). Extension and exhumation of the HP/LT rocks in the Hellenic forearc ridge. *American Journal of Science, 310*(1), 1-36.

McPhee, P. J., Altıner, D., & van Hinsbergen, D. J. J. (2018). First Balanced Cross Section Across the Taurides Fold-Thrust Belt: Geological Constraints on the Subduction History of the Antalya Slab in Southern Anatolia. *Tectonics*.

McPhee, P. J., Koç, A., & van Hinsbergen, D. J. J. (2022). Preparing the ground for plateau growth: Late Neogene Central Anatolian uplift in the context of orogenic and geodynamic evolution since the Cretaceous. *Tectonophysics, 822*, 229131.

McPhee, P. J., van Hinsbergen, D. J. J., & Thomson, S. (2019). Thermal history of the western Central Taurides fold-thrust belt: Implications for Cenozoic vertical motions of southern Central Anatolia. *Geosphere, 15*, 1927-1942.

Memiş, C., Göğüş, O. H., Uluocak, E. Ş., Pysklywec, R., Keskin, M., Şengör, A. C., & Topuz, G. (2020). Long wavelength progressive plateau uplift in Eastern Anatolia since 20 Ma: implications for the role of slab peel-Back and Break-off. *Geochemistry, Geophysics, Geosystems, 21*(2), e2019GC008726.

Mueller, M., Licht, A., Campbell, C., Ocakoğlu, F., Taylor, M., Burch, L., et al. (2019). Collision chronology along the İzmir-Ankara-Erzincan suture zone: Insights from the Sarıcakaya Basin, western Anatolia. *Tectonics, 38*(10), 3652-3674.

Mulcahy, S. R., Vervoort, J. D., & Renne, P. R. (2014). Dating subduction-zone metamorphism with combined garnet and lawsonite Lu–Hf geochronology. *Journal of Metamorphic Geology, 32*(5), 515-533. https://doi.org/10.1111/jmg.12092

Ocakoğlu, F., Hakyemez, A., Açıkalın, S., Özkan Altıner, S., Büyükmeriç, Y., Licht, A., et al. (2019). Chronology of subduction and collision along the İzmir-Ankara suture in Western Anatolia: records from the Central Sakarya Basin. *International Geology Review, 61*(10), 1244-1269.

Okay, A. (2002). Jadeite–chloritoid–glaucophane–lawsonite blueschists in north-west Turkey: unusually high P/T ratios in continental crust. *Journal of Metamorphic Geology, 20*(8), 757-768.

Okay, A. I. (2001). Stratigraphic and metamorphic inversions in the central Menderes Massif: a new structural model. *International Journal of Earth Sciences, 89*(4), 709-727.

Okay, A. I., Satir, M., Maluski, H., Siyako, M., Monie, P., Metzger, R., & Akyüz, S. (1996). Paleo-and Neo-Tethyan events in northwestern Turkey: geologic and geochronologic constraints. *World and Regional Geology*, 420-441.

Okay, A. I., & Whitney, D. L. (2010). Blueschists, eclogites, ophiolites and suture zones in northwest Turkey: a review and a field excursion guide. *Ofioliti, 35*(2), 131-172.
Önen, A. P. (2003). Neotethyan ophiolitic rocks of the Anatolides of NW Turkey and comparison with Tauride ophiolites. *Journal of the Geological Society, 160*, 947-962.
Önen, A. P., & Hall, R. (1993). Ophiolites and related metamorphic rocks from the Kütahya region, north-west Turkey. *Geological Journal, 160*, 947-962.
Özer, S., & Sözbilir, H. (2003). Presence and tectonic significance of Cretaceous rudist species in the so-called Permo-Carboniferous Göktepe Formation, central Menderes metamorphic massif, western Turkey. *International Journal of Earth Sciences, 92*(3), 397-404. https://doi.org/10.1007/s00531-003-0333-z
Ozgenc, I., & Ilbeyli, N. (2008). Petrogenesis of the Late Cenozoic Egrigöz pluton in western Anatolia, Turkey: implications for magma genesis and crustal processes. *International Geology Review, 50*(4), 375-391.
Palin, R. M., Reuber, G. S., White, R. W., Kaus, B. J., & Weller, O. M. (2017). Subduction metamorphism in the Himalayan ultrahigh-pressure Tso Morari massif: an integrated geodynamic and petrological modelling approach. *Earth and Planetary Science Letters, 467*, 108-119.
Parlak, O. (2016). The tauride ophiolites of Anatolia (Turkey): A review. *Journal of Earth Science, 27*(6), 901-934.
Peillod, A., Ring, U., Glodny, J., & Skelton, A. (2017). An Eocene/Oligocene blueschist-/greenschist facies P–T loop from the Cycladic Blueschist Unit on Naxos Island, Greece: Deformation-related re-equilibration vs. thermal relaxation. *Journal of Metamorphic Geology, 35*(7), 805-830.
Platt, J. (1986). Dynamics of orogenic wedges and the uplift of high-pressure metamorphic rocks. *Geological Society of America Bulletin, 97*(9), 1037-1053.
Platt, J. P., & Vissers, R. L. M. (1989). Extensional collapse of thickened continental lithosphere: A working hypothesis for the Alboran Sea and Gibraltar arc. *Geology, 17*(6), 540-543.

Plunder, A., Agard, P., Chopin, C., & Okay, A. I. (2013). Geodynamics of the Tavşanlı zone, western Turkey: Insights into subduction/obduction processes. *Tectonophysics, 608*, 884-903.
Plunder, A., Thieulot, C., & van Hinsbergen, D. J. J. (2018). The effect of obliquity on temperature in subduction zones: insights from 3-D numerical modeling. *Solid Earth, 9*(3), 759-776.
Pourteau, A., Candan, O., & Oberhänsli, R. (2010). High-pressure metasediments in central Turkey: Constraints on the Neotethyan closure history. *Tectonics, 29*(5), n/a-n/a.
Pourteau, A., Scherer, E. E., Schorn, S., Bast, R., Schmidt, A., & Ebert, L. (2019). Thermal evolution of an ancient subduction interface revealed by Lu–Hf garnet geochronology, Halilbağı Complex (Anatolia). *Geoscience Frontiers, 10*, 127-148.
Pourteau, A., Sudo, M., Candan, O., Lanari, P., Vidal, O., & Oberhänsli, R. (2013). Neotethys closure history of Anatolia: insights from 40Ar-39Ar geochronology andP-Testimation in high-pressure metasedimentary rocks. *Journal of Metamorphic Geology, 31*(6), 585-606.
Rahl, J., Anderson, K., Brandon, M., & Fassoulas, C. (2005). Raman spectroscopic carbonaceous material thermometry of low-grade metamorphic rocks: Calibration and application to tectonic exhumation in Crete, Greece. *Earth and Planetary Science Letters, 240*(2), 339-354.
Replumaz, A., Negredo, A. M., Villaseñor, A., & Guillot, S. (2010). Indian continental subduction and slab break-off during Tertiary collision. *Terra Nova, 22*, 290-296.

Rimmelé, G., Oberhänsli, R., Goffé, B., Jolivet, L., Candan, O., & Çetinkaplan, M. (2003). First evidence of high-pressure metamorphism in the "Cover Series" of the southern Menderes Massif. Tectonic and metamorphic implications for the evolution of SW Turkey. *Lithos, 71*(1), 19-46.

Ring, U., & Collins, A. S. (2005). U-Pb SIMS dating of synkinematic granites: timing of core-complex formation in the northern Anatolide belt of western Turkey. *Journal of the Geological Society, 162*(2), 289-298.

Ring, U., Glodny, J., Will, T., & Thomson, S. (2007a). An Oligocene extrusion wedge of blueschist-facies nappes on Evia, Aegean Sea, Greece: implications for the early exhumation of high-pressure rocks. *Journal of the Geological Society, 164*(3), 637-652.

Ring, U., & Layer, P. W. (2003). High-pressure metamorphism in the Aegean, eastern Mediterranean: Underplating and exhumation from the Late Cretaceous until the Miocene to Recent above the retreating Hellenic subduction zone. *Tectonics, 22*(3)

Ring, U., Layer, P. W., & Reischmann, T. (2001). Miocene high-pressure metamorphism in the Cyclades and Crete, Aegean Sea, Greece: Evidence for large-magnitude displacement on the Cretan detachment. *Geology, 29*(5), 395-398.

Ring, U., Will, T., Glodny, J., Kumerics, C., Gessner, K., Thomson, S., et al. (2007b). Early exhumation of high-pressure rocks in extrusion wedges: Cycladic blueschist unit in the eastern Aegean, Greece, and Turkey. *Tectonics, 26*(2), n/a-n/a.

Ring, U., & Yngwe, F. (2018). "To Be, or Not to Be, That Is the Question"—The Cretan Extensional Detachment, Greece. *Tectonics, 37*, 3069-3084.

Romano, S. S., Dörr, W., & Zulauf, G. (2004). Cambrian granitoids in pre-Alpine basement of Crete (Greece): evidence from U-Pb dating of zircon. *International Journal of Earth Sciences, 93*(5), 844-859.

Schmid, S. M., Bernoulli, D., Fügenschuh, B., Georgiev, N., Kounov, A., Matenco, L., et al. (2020). Tectonic units of the Alpine collision zone between Eastern Alps and Western Turkey. *Gondwana Research, 78*, 308-374.

Schmid, S.M., Scharf, A., Handy, M.R. and Rosenberg, C.L (2013). The Tauern Window (Eastern Alps, Austria): a new tectonic map, with cross-sections and a tectonometamorphic synthesis. *Swiss Journal of Geosciences, 106(1)*, 1-32.

Schmidt, A., Pourteau, A., Candan, O., & Oberhänsli, R. (2015). Lu–Hf geochronology on cm-sized garnets using microsampling: New constraints on garnet growth rates and duration of metamorphism during continental collision (Menderes Massif, Turkey). *Earth and Planetary Science Letters, 432*, 24-35.

Searle, M. P., & Lamont, T. N. (2020). Compressional metamorphic core complexes, low-angle normal faults and extensional fabrics in compressional tectonic settings. *Geological Magazine, 157*(1), 101-118.

Seaton, N. C. A., Teyssier, C., Whitney, D. L., & Heizler, M. T. (2014). Quartz and calcite microfabric transitions in a pressure and temperature gradient, Sivrihisar, Turkey. *Geodinamica Acta, 26*(3-4), 191-206.

Şengör, A. M. C., & Yilmaz, Y. (1981). Tethyan evolution of Turkey: A plate tectonic approach. *Tectonophysics, 75*(3), 181-241.

Seyitoğlu, G., Isik, V., Gürbüz, E., & Gürbüz, A. (2017). The discovery of a low-angle normal fault in the Taurus Mountains: the İvriz detachment and implications concerning the Cenozoic geology of southern Turkey*. *Turkish Journal of Earth Sciences, 26*, 189-205.

Skelton, A., Peillod, A., Glodny, J., Klonowska, I., Månbro, C., Lodin, K., & Ring, U. (2019). Preservation of high-P rocks coupled to rock composition and the absence of metamorphic fluids. *Journal of Metamorphic Geology, 37*(3), 359-381.

Smit, M. A., Hacker, B. R., & Lee, J. (2014). Tibetan garnet records early Eocene initiation of thickening in the Himalaya. *Geology, 42*(7), 591-594.

Smye, A. J., Bickle, M. J., Holland, T. J., Parrish, R. R., & Condon, D. J. (2011). Rapid formation and exhumation of the youngest Alpine eclogites: a thermal conundrum to Barrovian metamorphism. *Earth and Planetary Science Letters, 306*(3-4), 193-204.

Sotiropoulos, S., Kamberis, E., Triantaphyllou, M. V., & Doutsos, T. (2003). Thrust sequences in the central part of the External Hellenides. *Geological Magazine, 140*(6), 661-668.

Spakman, W., & Hall, R. (2010). Surface deformation and slab–mantle interaction during Banda arc subduction rollback. *Nature Geoscience, 3*(8), 562-566.

St-Onge, M. R., Searle, M. P., & Wodicka, N. (2006). Trans-Hudson Orogen of North America and Himalaya-Karakoram-Tibetan Orogen of Asia: Structural and thermal characteristics of the lower and upper plates. *Tectonics, 25*(4).

Stübner, K., Grujic, D., Parrish, R. R., Roberts, N. M. W., Kronz, A., Wooden, J., & Ahmad, T. (2014). Monazite geochronology unravels the timing of crustal thickening in NW Himalaya. *Lithos, 210-211*, 111-128.

Tezel, T., Shibutani, T., & Kaypak, B. (2013). Crustal thickness of Turkey determined by receiver function. *Journal of Asian Earth Sciences, 75*, 36-45.

Theye, T., Seidel, E., & Vidal, O. (1992). Carpholite, sudoite, and chloritoid in low-grade high-pressure metapelites from Crete and the Peloponnese, Greece. *European Journal of Mineralogy, 4*(3), 487-507.

Thomson, S. N., Stöckhert, B., & Brix, M. R. (1999). Miocene high-pressure metamorphic rocks of Crete, Greece: rapid exhumation by buoyant escape. *Geological Society, London, Special Publications, 154*(1), 87-107.

Tirel, C., Brun, J. P., Burov, E., Wortel, M. J. R., & Lebedev, S. (2013). A plate tectonics oddity: Caterpillar-walk exhumation of subducted continental crust. *Geology, 41*(5), 555-558.

Tirel, C., Gueydan, F., Tiberi, C., & Brun, J.-P. (2004). Aegean crustal thickness inferred from gravity inversion. Geodynamical implications. *Earth and Planetary Science Letters, 228*(3-4), 267-280.

Tomaschek, F. (2003). Zircons from Syros, Cyclades, Greece--Recrystallization and Mobilization of Zircon During High-Pressure Metamorphism. *Journal of Petrology, 44*(11), 1977-2002.

Toussaint, G., Burov, E., & Avouac, J. P. (2004). Tectonic evolution of a continental collision zone: A thermomechanical numerical model. *Tectonics, 23*(6).

Tual, L., Smit, M. A., Cutts, J., Kooijman, E., Kielman-Schmitt, M., Majka, J., & Foulds, I. (2022). Rapid, paced metamorphism of blueschists (Syros, Greece) from laser-based zoned Lu-Hf garnet chronology and LA-ICPMS trace element mapping. *Chemical Geology, 607*, 121003.

Uunk, B., Brouwer, F., de Paz-Álvarez, M., van Zuilen, K., Huybens, R., van't Veer, R., & Wijbrans, J. (2022). Consistent detachment of supracrustal rocks from a fixed subduction depth in the Cyclades. *Earth and Planetary Science Letters, 584*, 117479.

van de Lagemaat, S. H., Swart, M. L., Vaes, B., Kosters, M. E., Boschman, L. M., Burton-Johnson, A., et al. (2021). Subduction initiation in the Scotia Sea region and opening of the Drake Passage: When and why? *Earth-Science Reviews*, 103551.

van Hinsbergen, D. J. J. (2022). Indian Plate paleogeography, subduction, and horizontal underthrusting below Tibet: paradoxes, controvercies, and opportunities. *National Science Review, 9*(8), nwac074.
van Hinsbergen, D. J. J., Hafkenscheid, E., Spakman, W., Meulenkamp, J. E., & Wortel, R. (2005a). Nappe stacking resulting from subduction of oceanic and continental lithosphere below Greece. *Geology, 33*(4).
van Hinsbergen, D. J. J., Kaymakci, N., Spakman, W., & Torsvik, T. H. (2010). Reconciling the geological history of western Turkey with plate circuits and mantle tomography. *Earth and Planetary Science Letters, 297*(3-4), 674-686.
van Hinsbergen, D. J. J., Lippert, P. C., Li, S., Huang, W., Advokaat, E. L., & Spakman, W. (2019). Reconstructing Greater India: Paleogeographic, kinematic, and geodynamic perspectives. *Tectonophysics, 760*, 69-94.
van Hinsbergen, D. J. J., Maffione, M., Plunder, A., Kaymakci, N., Ganerød, M., Hendriks, B. W. H., et al. (2016). Tectonic evolution and paleogeography of the Kırşehir Block and the Central Anatolian Ophiolites, Turkey. *Tectonics, 35*, 983-1014.
van Hinsbergen, D. J. J., & Schmid, S. M. (2012). Map view restoration of Aegean-West Anatolian accretion and extension since the Eocene. *Tectonics, 31*(5), n/a-n/a.
van Hinsbergen, D. J. J., & Schouten, T. L. A. (2021). Deciphering paleogeography from orogenic architecture: constructing orogens in a future supercontinent as thought experiment. *American Journal of Science, 321*, 955-1031.
van Hinsbergen, D. J. J., Steinberger, B., Guilmette, C., Maffione, M., Gürer, D., Peters, K., et al. (2021). A record of plume-induced plate rotation triggering seafloor spreading and subduction initiation. *Nature Geoscience, 14*, 626-630.
van Hinsbergen, D. J. J., Torsvik, T., Schmid, S. M., Matenco, L., Maffione, M., Vissers, R. L. M., et al. (2020). Orogenic architecture of the Mediterranean region and kinematic reconstruction of its tectonic evolution since the Triassic. *Gondwana Research, 81*, 79-229.
van Hinsbergen, D. J. J., van der Meer, D. G., Zachariasse, W. J., & Meulenkamp, J. E. (2006). Deformation of western Greece during Neogene clockwise rotation and collision with Apulia. *International Journal of Earth Sciences, 95*(3), 463-490.
van Hinsbergen, D. J. J., Zachariasse, W. J., Wortel, M. J. R., & Meulenkamp, J. E. (2005b). Underthrusting and exhumation: A comparison between the External Hellenides and the "hot" Cycladic and "cold" South Aegean core complexes (Greece). *Tectonics, 24*(2), n/a-n/a.
Wardle, R. J., James, D. T., Scott, D. J., & Hall, J. (2002). The southeastern Churchill Province: synthesis of a Paleoproterozoic transpressional orogen. *Canadian Journal of Earth Sciences, 39*(5), 639-663.
Webb, A. A. G., Guo, H., Clift, P. D., Husson, L., Müller, T., Costantino, D., et al. (2017). The Himalaya in 3D: Slab dynamics controlled mountain building and monsoon intensification. *Lithosphere*.
Weller, O. M., St-Onge, M. R., Waters, D. J., Rayner, N., Searle, M. P., Chung, S. L., et al. (2013). Quantifying Barrovian metamorphism in the Danba Structural Culmination of eastern Tibet. *Journal of Metamorphic Geology, 31*(9), 909-935.
Whitney, D. L., & Bozkurt, E. (2002). Metamorphic history of the southern Menderes massif, western Turkey. *GSA Bulletin, 114*(7), 829-838.

Whitney, D. L., & Dilek, Y. (1998). Metamorphism during Alpine Crustal Thickening and Extension in Central Anatolia, Turkey: the Niğde Metamorphic Core Complex. *Journal of Petrology, 39*(7), 1385-1403.

Whitney, D. L., & Hamilton, M. A. (2004). Timing of high-grade metamorphism in central Turkey and the assembly of Anatolia. *Journal of the Geological Society, 161*(5), 823-828.
Whitney, D. L., Teyssier, C., Fayon, A. K., Hamilton, M. A., & Heizler, M. (2003). Tectonic controls on metamorphism, partial melting, and intrusion: timing and duration of regional metamorphism and magmatism in the Niğde Massif, Turkey. *Tectonophysics, 376*(1-2), 37-60.
Wolfe, O. M., Spear, F. S., Thomas, J. B., Hasegawa, E. M., Libby, G. T., & Cheney, J. T. (2023). Pressure–temperature evolution of the basement and cover sequences on Ios, Greece: Evidence for subduction of the Hercynian basement. *Journal of Metamorphic Geology, 41*(8), 1119-1141.
Zachariasse, W. J., van Hinsbergen, D. J. J., & Fortuin, A. R. (2011). Formation and fragmentation of a late Miocene supradetachment basin in central Crete: implications for exhumation mechanisms of high-pressure rocks in the Aegean forearc. *Basin Research, 23*(6), 678-701.

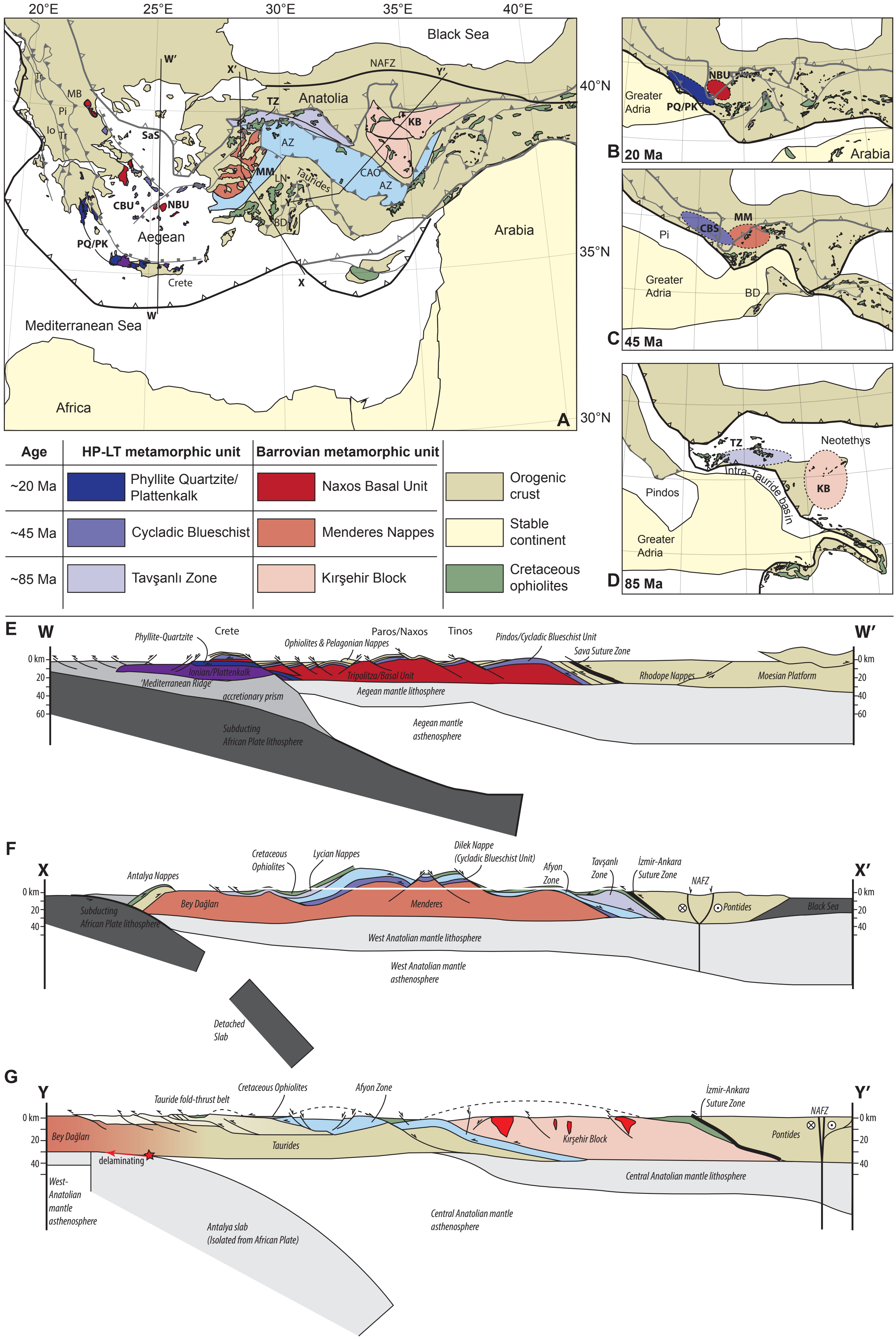

20°E
25°E
30°E
35°E
40°E
40°N
35°N
30°N
Black Sea
NAFZ
Anatolia
TZ
KB
AZ
CAO
MM
LN
Taurides
BD
SaS
MB
Pi
Io
Tr
CBU
NBU
PQ/PK
Aegean
Crete
Mediterranean Sea
Arabia
Africa
W
W'
X
X'
Y
Y'
A
Greater Adria
NBU
PQ/PK
Arabia
B 20 Ma
MM
CBS
Pi
Greater Adria
BD
C 45 Ma
TZ
Neotethys
Intra-Tauride basin
KB
Pindos
Greater Adria
D 85 Ma
Age
HP-LT metamorphic unit
Barrovian metamorphic unit
~20 Ma
Phyllite Quartzite/ Plattenkalk
Naxos Basal Unit
Orogenic crust
~45 Ma
Cycladic Blueschist
Menderes Nappes
Stable continent
~85 Ma
Tavşanlı Zone
Kırşehir Block
Cretaceous ophiolites
E
Phyllite-Quartzite
Crete
Ophiolites & Pelagonian Nappes
Paros/Naxos
Tinos
Pindos/Cycladic Blueschist Unit
Sava Suture Zone
0 km
20
40
60
Ionian/Plattenkalk
'Mediterranean Ridge'
accretionary prism
Tripolitza/Basal Unit
Aegean mantle lithosphere
Rhodope Nappes
Moesian Platform
Subducting African Plate lithosphere
Aegean mantle asthenosphere
F
Antalya Nappes
Cretaceous Ophiolites
Lycian Nappes
Dilek Nappe (Cycladic Blueschist Unit)
Afyon Zone
Tavşanlı Zone
İzmir-Ankara Suture Zone
NAFZ
Subducting African Plate lithosphere
Bey Dağları
Menderes
Pontides
Black Sea
West Anatolian mantle lithosphere
West Anatolian mantle asthenosphere
Detached Slab
G
Tauride fold-thrust belt
Cretaceous Ophiolites
Afyon Zone
İzmir-Ankara Suture Zone
NAFZ
Bey Dağları
Taurides
Kırşehir Block
Pontides
delaminating
Central Anatolian mantle lithosphere
West-Anatolian mantle asthenosphere
Antalya slab (Isolated from African Plate)
Central Anatolian mantle asthenosphere

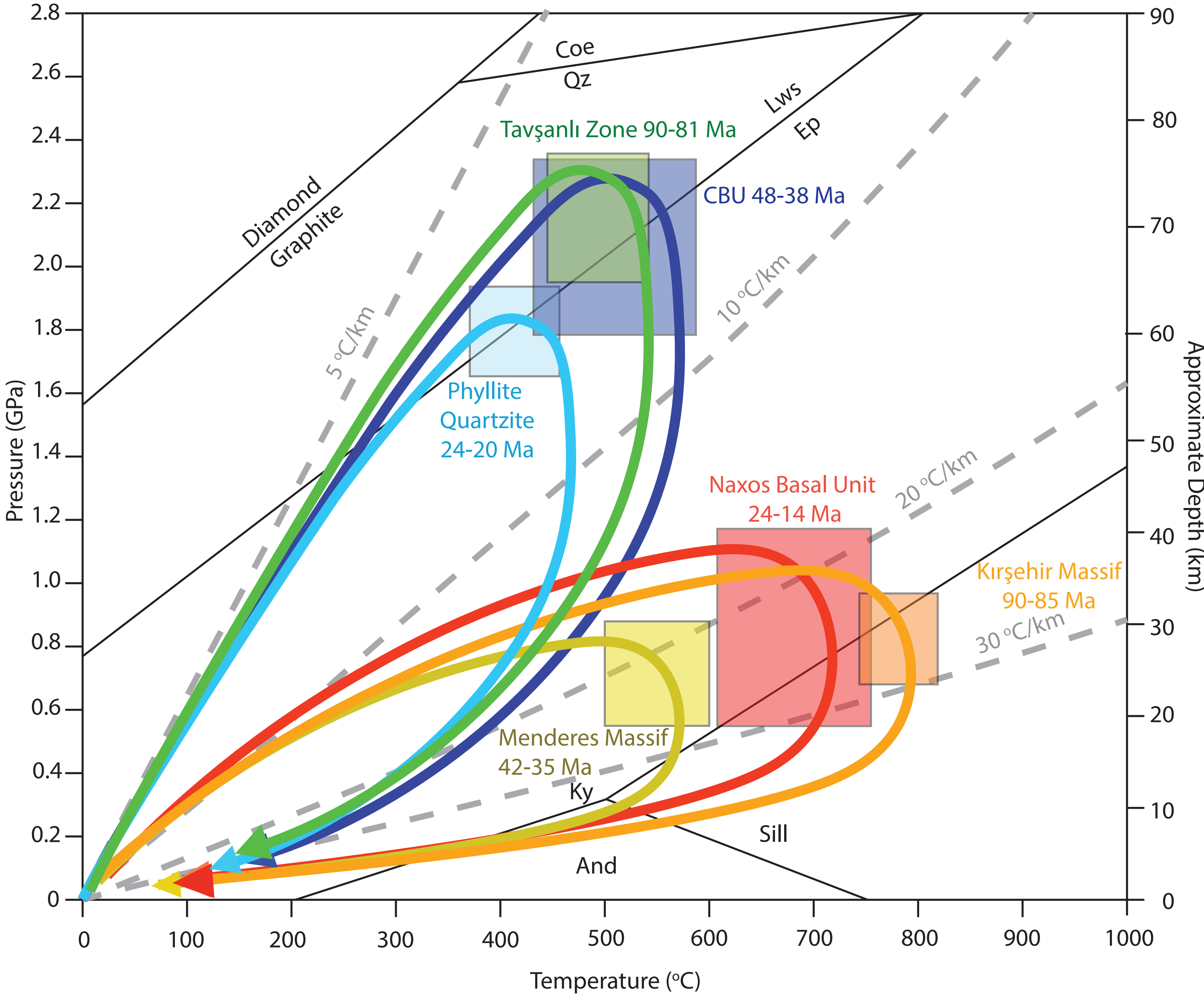
Pressure (GPa)
Approximate Depth (km)
Temperature (°C)
Coe
Qz
Diamond
Graphite
Lws
Ep
5 °C/km
10 °C/km
20 °C/km
30 °C/km
Tavşanlı Zone 90-81 Ma
CBU 48-38 Ma
Phyllite
Quartzite
24-20 Ma
Naxos Basal Unit
24-14 Ma
Kırşehir Massif
90-85 Ma
Menderes Massif
42-35 Ma
Ky
Sill
And

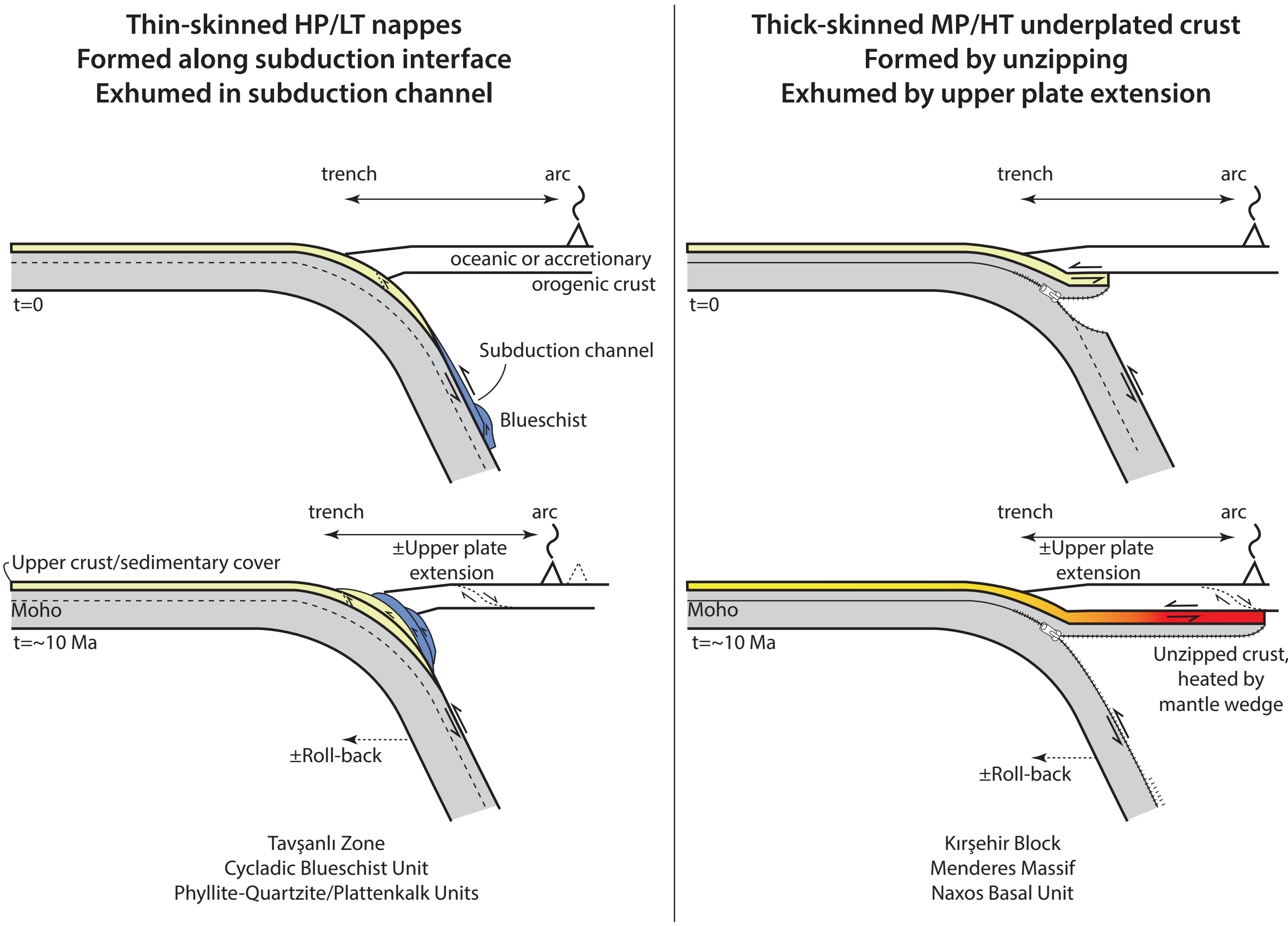
Thin-skinned HP/LT nappes
Formed along subduction interface
Exhumed in subduction channel
trench
arc
oceanic or accretionary
orogenic crust
t=0
Subduction channel
Blueschist
trench
arc
±Upper plate
extension
Upper crust/sedimentary cover
Moho
t=~10 Ma
±Roll-back
Tavşanlı Zone
Cycladic Blueschist Unit
Phyllite-Quartzite/Plattenkalk Units
Thick-skinned MP/HT underplated crust
Formed by unzipping
Exhumed by upper plate extension
trench
arc
t=0
trench
arc
±Upper plate
extension
Moho
t=~10 Ma
Unzipped crust,
heated by
mantle wedge
±Roll-back
Kırşehir Block
Menderes Massif
Naxos Basal Unit

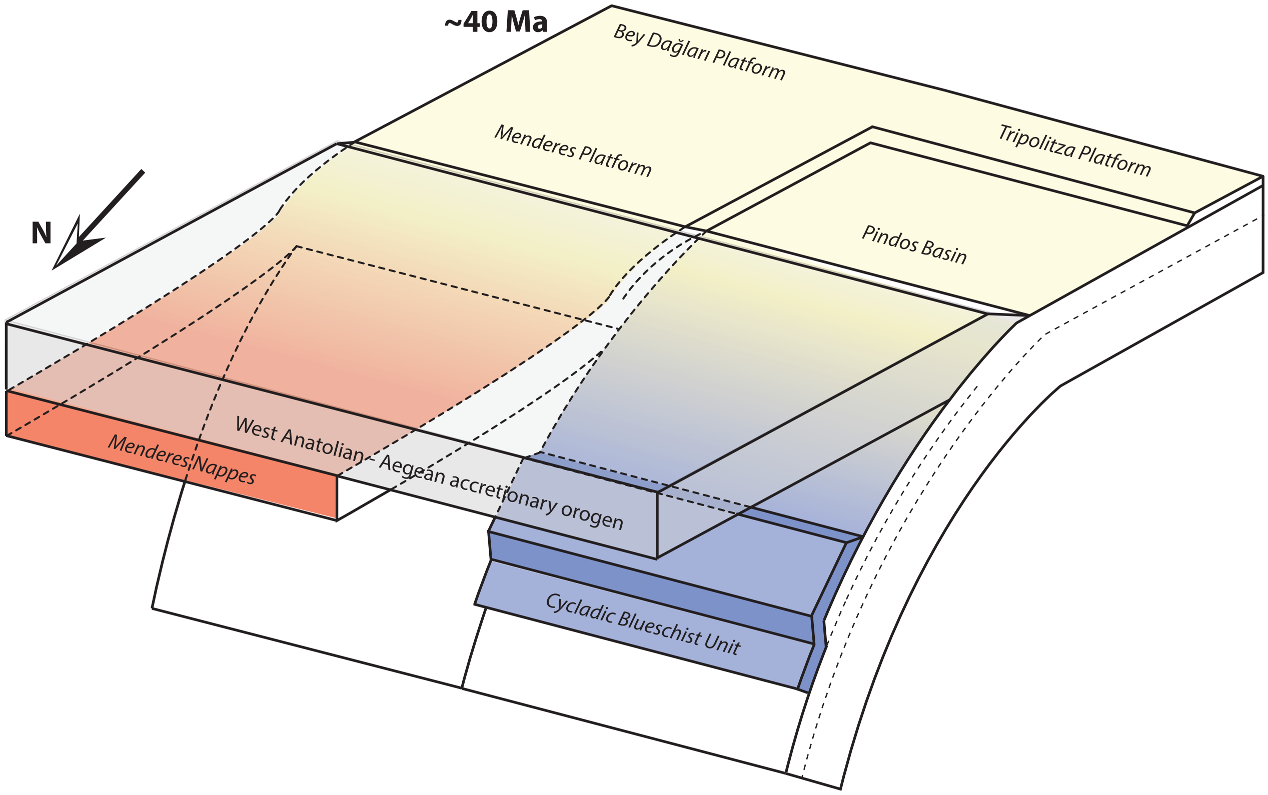
~40 Ma
N
Bey Dağları Platform
Menderes Platform
Tripolitza Platform
Pindos Basin
West Anatolian - Aegean accretionary orogen
Menderes Nappes
Cycladic Blueschist Unit

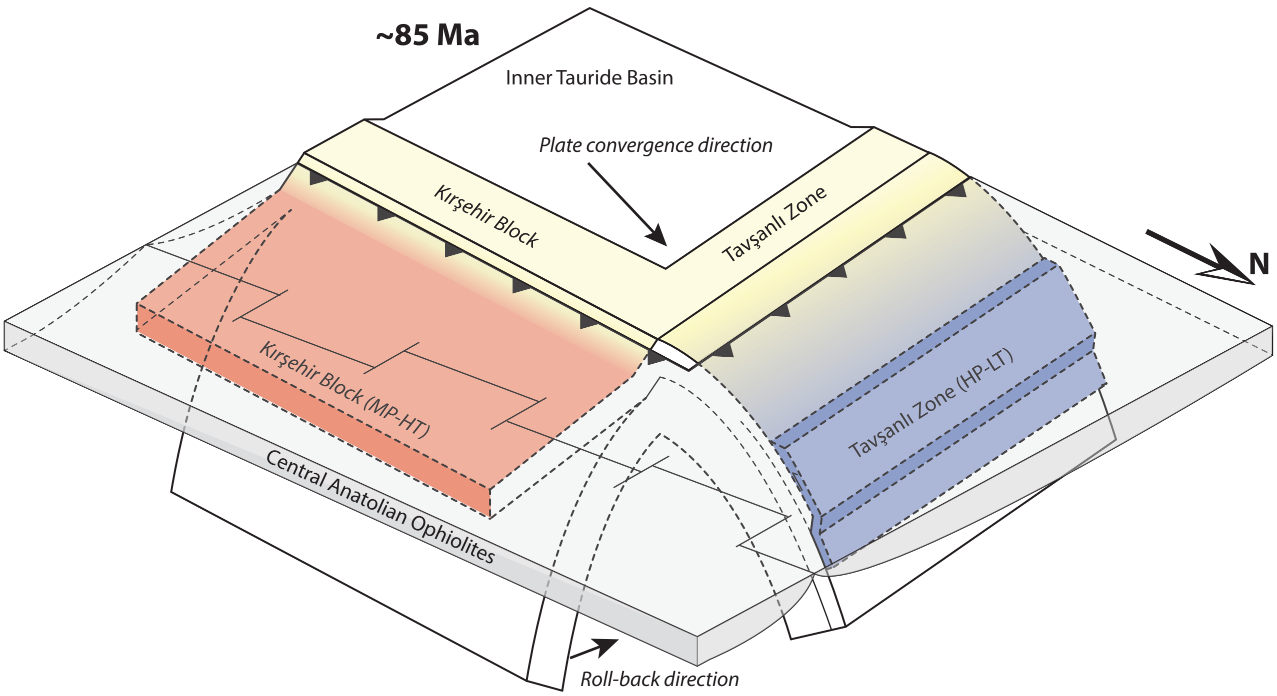
~85 Ma
Inner Tauride Basin
Plate convergence direction
Kırşehir Block
Tavşanlı Zone
N
Kırşehir Block (MP-HT)
Tavşanlı Zone (HP-LT)
Central Anatolian Ophiolites
Roll-back direction

**Simultaneous formation
Phyllite-Quartzite HP-LT and
Naxos Basal Unit MP-HT nappes**

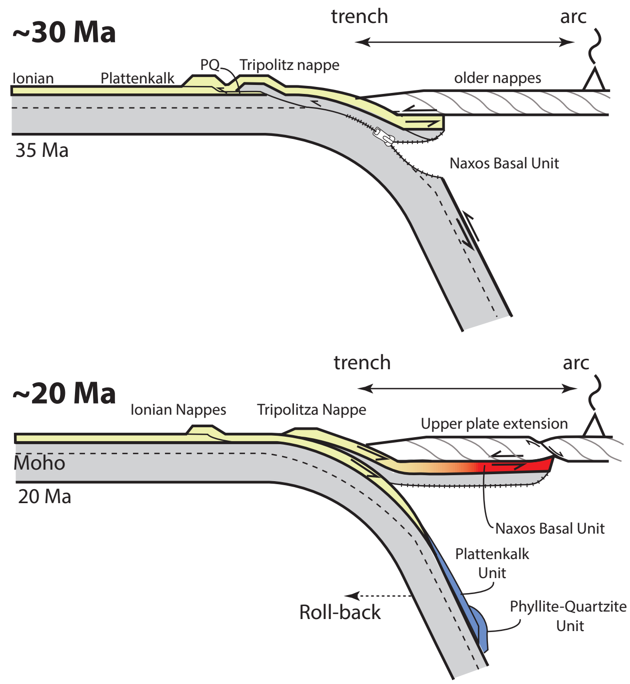

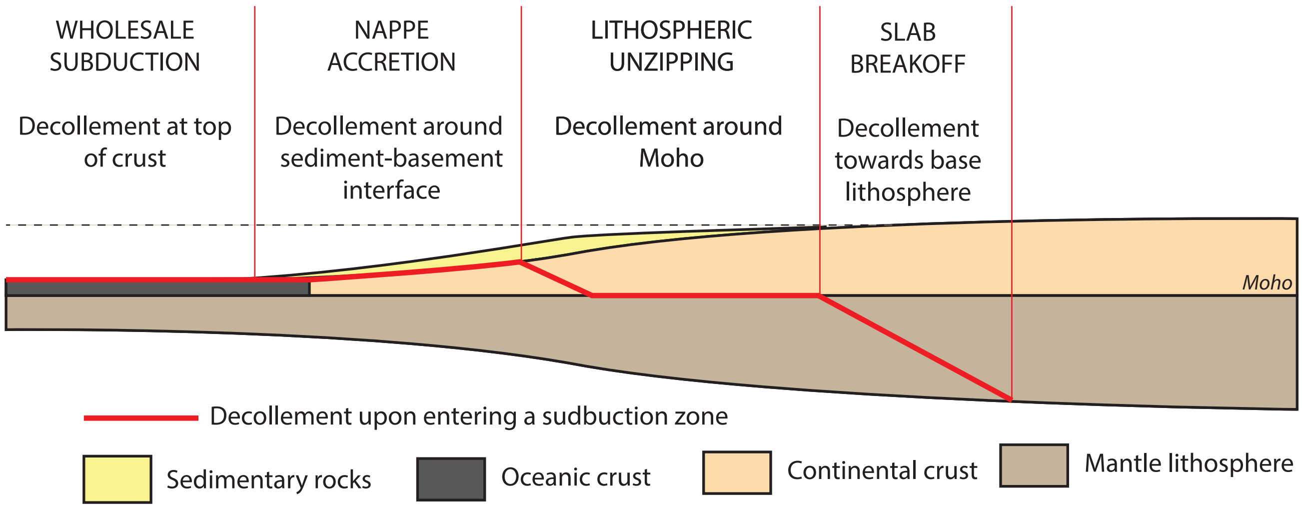
WHOLESALE SUBDUCTION
Decollement at top of crust
NAPPE ACCRETION
Decollement around sediment-basement interface
LITHOSPHERIC UNZIPPING
Decollement around Moho
SLAB BREAKOFF
Decollement towards base lithosphere
Moho
Decollement upon entering a sudbuction zone
Sedimentary rocks
Oceanic crust
Continental crust
Mantle lithosphere

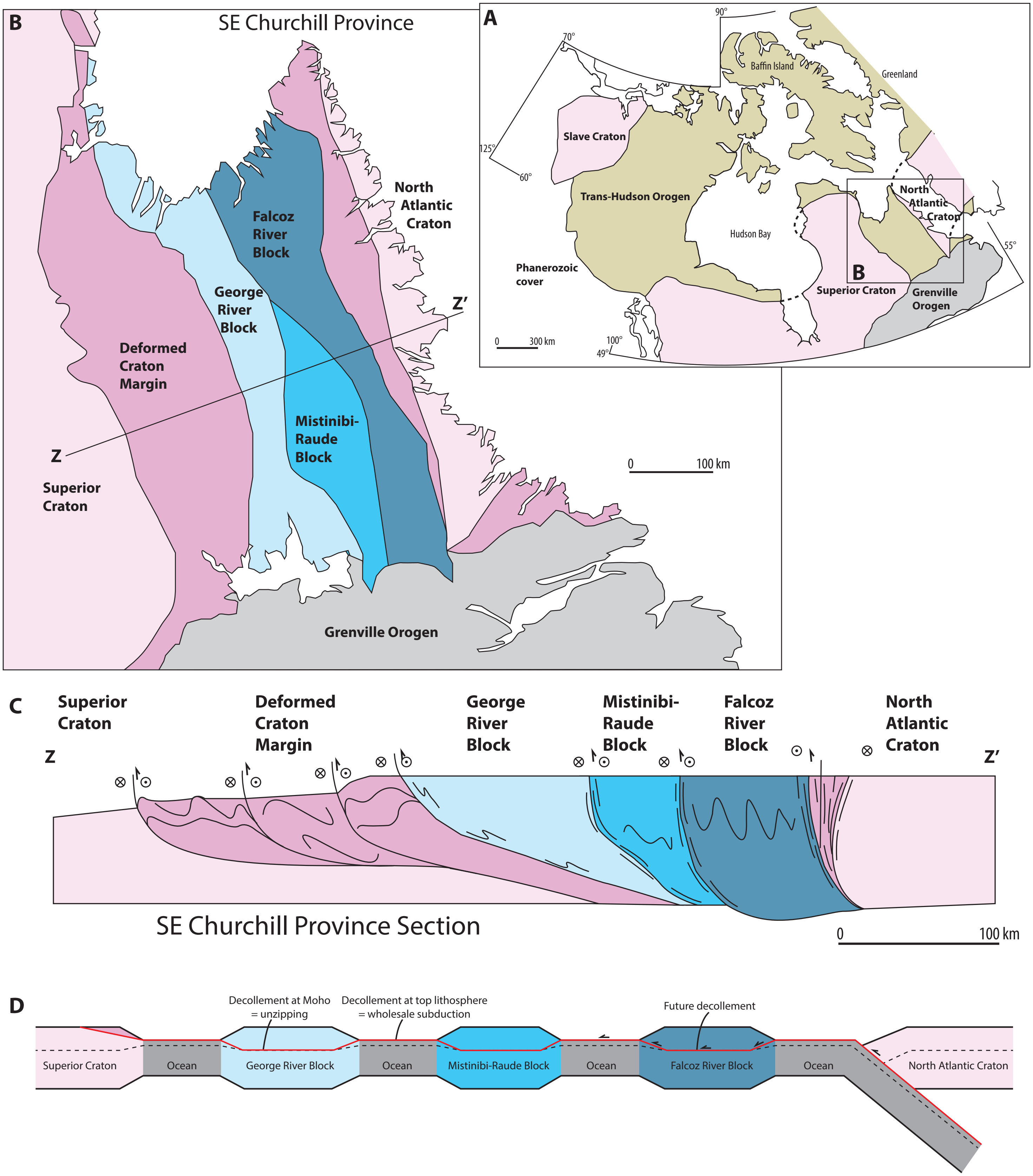
B
SE Churchill Province
North Atlantic Craton
Falcoz River Block
George River Block
Deformed Craton Margin
Mistinibi-Raude Block
Z
Z′
Superior Craton
0 100 km
Grenville Orogen
A
90°
70°
Baffin Island
Greenland
Slave Craton
125°
60°
Trans-Hudson Orogen
North Atlantic Craton
Hudson Bay
55°
Phanerozoic cover
B
Superior Craton
Grenville Orogen
0 300 km
100°
49°
C
Superior Craton
Deformed Craton Margin
George River Block
Mistinibi-Raude Block
Falcoz River Block
North Atlantic Craton
Z
Z′
SE Churchill Province Section
0 100 km
D
Decollement at Moho
= unzipping
Decollement at top lithosphere
= wholesale subduction
Future decollement
Superior Craton
Ocean
George River Block
Ocean
Mistinibi-Raude Block
Ocean
Falcoz River Block
Ocean
North Atlantic Craton